

EUR 2714.e

EUROPEAN ATOMIC ENERGY COMMUNITY - EURATOM

**A MEASUREMENT OF THE HYPERFINE STRUCTURE
OF THE THERMAL FLUX DISTRIBUTION IN THE UC
CLUSTERED FUEL ELEMENT ESSOR C-2- φ**

by

S. GUARDINI and G.F. PIPITONE



1966

ORGEL Program

**Joint Nuclear Research Center
Ispra Establishment - Italy**

**Reactor Physics Department
Experimental Neutron Physics**

LEGAL NOTICE

This document was prepared under the sponsorship of the Commission of the European Atomic Energy Community (EURATOM).

Neither the EURATOM Commission, its contractors nor any person acting on their behalf :

Make any warranty or representation, express or implied, with respect to the accuracy, completeness, or usefulness of the information contained in this document, or that the use of any information, apparatus, method, or process disclosed in this document may not infringe privately owned rights; or

Assume any liability with respect to the use of, or for damages resulting from the use of any information, apparatus, method or process disclosed in this document.

This report is on sale at the addresses listed on cover page 4.

at the price of	FF 6,-	FB 60,-	DM 4.80	Lit. 750	Fl. 4.30
-----------------	--------	---------	---------	----------	----------

When ordering, please quote the EUR number and the title, which are indicated on the cover of each report.

Printed by Smeets
Brussels, March 1966

This document was reproduced on the basis of the best available copy.

EUR 2714.e

A MEASUREMENT OF THE HYPERFINE STRUCTURE OF THE THERMAL FLUX DISTRIBUTION IN THE UC CLUSTERED FUEL ELEMENT ESSOR C-2- φ by S. GUARDINI and G.F. PIPITONE

European Atomic Energy Community - EURATOM
ORGEL Program

Joint Nuclear Research Center - Ispra Establishment (Italy)
Reactor Physics Department - Experimental Neutron Physics
Brussels, March 1966 - 46 Pages - 24 Figures - FB 60

The detailed hyperfine structure distribution of the thermal flux in the clustered fuel element of the first charge of the ESSOR reactor has

EUR 2714.e

A MEASUREMENT OF THE HYPERFINE STRUCTURE OF THE THERMAL FLUX DISTRIBUTION IN THE UC CLUSTERED FUEL ELEMENT ESSOR C-2- φ by S. GUARDINI and G.F. PIPITONE

European Atomic Energy Community - EURATOM
ORGEL Program

Joint Nuclear Research Center - Ispra Establishment (Italy)
Reactor Physics Department - Experimental Neutron Physics
Brussels, March 1966 - 46 Pages - 24 Figures - FB 60

The detailed hyperfine structure distribution of the thermal flux in the clustered fuel element of the first charge of the ESSOR reactor has

EUR 2714.e

A MEASUREMENT OF THE HYPERFINE STRUCTURE OF THE THERMAL FLUX DISTRIBUTION IN THE UC CLUSTERED FUEL ELEMENT ESSOR C-2- φ by S. GUARDINI and G.F. PIPITONE

European Atomic Energy Community - EURATOM
ORGEL Program

Joint Nuclear Research Center - Ispra Establishment (Italy)
Reactor Physics Department - Experimental Neutron Physics
Brussels, March 1966 - 46 Pages - 24 Figures - FB 60

The detailed hyperfine structure distribution of the thermal flux in the clustered fuel element of the first charge of the ESSOR reactor has

been measured by activation of Dy detectors. This element consists of a cluster of 4 uranium carbide rods, organic cooled, which is moderated by D_2O . Several degrees of poisoning of the element (corresponding to the increasing burn-up) have been investigated. The measured flux distributions have been compared with the corresponding distributions obtained by an analytical expression of empirical nature.

been measured by activation of Dy detectors. This element consists of a cluster of 4 uranium carbide rods, organic cooled, which is moderated by D_2O . Several degrees of poisoning of the element (corresponding to the increasing burn-up) have been investigated. The measured flux distributions have been compared with the corresponding distributions obtained by an analytical expression of empirical nature.

been measured by activation of Dy detectors. This element consists of a cluster of 4 uranium carbide rods, organic cooled, which is moderated by D_2O . Several degrees of poisoning of the element (corresponding to the increasing burn-up) have been investigated. The measured flux distributions have been compared with the corresponding distributions obtained by an analytical expression of empirical nature.

EUR 2714.e

EUROPEAN ATOMIC ENERGY COMMUNITY - EURATOM

**A MEASUREMENT OF THE HYPERFINE STRUCTURE
OF THE THERMAL FLUX DISTRIBUTION IN THE UC
CLUSTERED FUEL ELEMENT ESSOR C-2- φ**

by

S. GUARDINI and G.F. PIPITONE



1966

ORGEL Program

**Joint Nuclear Research Center
Ispra Establishment - Italy**

**Reactor Physics Department
Experimental Neutron Physics**

SUMMARY

The detailed hyperfine structure distribution of the thermal flux in the clustered fuel element of the first charge of the ESSOR reactor has been measured by activation of Dy detectors. This element consists of a cluster of 4 uranium carbide rods, organic cooled, which is moderated by D_2O . Several degrees of poisoning of the element (corresponding to the increasing burn-up) have been investigated. The measured flux distributions have been compared with the corresponding distributions obtained by an analytical expression of empirical nature.

INTRODUCTION

A systematic experimental investigation of the hyperfine structure distribution of the thermal flux inside organic cooled, D_2O moderated, U and UC clustered fuel elements of various geometries, has been carried out in the past three years by the Experimental Neutron Physics Service at CCR Ispra, within the framework of the ORGEL Project (1, 2, 3).

Besides being of obvious interest for reactor physics studies, the hyperfine structure distribution of the thermal flux represents the relative heat source distribution in the fuel element, and has a direct bearing on the determination of the heat transfer to the coolant medium, as well as providing the information needed for mechanical deformation studies of the rods in the cluster.

It is reminded that the direct calculation of the hyperfine structure of the thermal flux in ORGEL-type fuel elements presents several difficulties, due mainly to the uncertainty in the values of the pertinent nuclear constants of the organic compound used as the coolant and to the complexity of the cluster geometries.

The present report describes a measurement of the hyperfine structure of the thermal flux of the 4-rod UC clustered fuel element foreseen for the first charge of ESSOR, a material testing reactor under construction at CCR Ispra. Several degrees of burn-up of the fuel element were simulated by various poisons concentrated on the axis of the cluster. A modified version of the element, with characteristics closer to those of an ORGEL power reactor fuel element, was also investigated.

Manuscript received on January 26, 1966.

The experimental technique used was essentially the same as that previously described (1, 2, 3), to which reference is made throughout the present report; however several details of the method were modified in order to increase the accuracy of the results.

EXPERIMENTAL DETAILS

The spatial distribution of the thermal flux in the fuel elements investigated was measured by the activation technique, using Dy^{164} as the thermal flux detector.

The fuel elements were irradiated in the critical facility AQUILON II, a D_2O moderated assembly at CEN Saclay (4), at the position of minimum flux variation (both radially and axially), in a central cell of the lattice.

The lattice of AQUILON II at the time of this experiment consisted of natural U rods, 29.2 mm in diameter and 2 m long, canned by Al, arranged in a square array with a 210 mm pitch (rod-to-rod). In order to generate around the measuring fuel element a zone with a space and energy distribution of the neutron flux similar to that existing in a full lattice of the elements investigated, 23 elements from the central portion of the AQUILON II lattice were replaced by 23 clustered fuel elements, each consisting of 19 Al-clad UO_2 rods (dia. 16.2 mm, length 2 m) arranged inside an hexagonal Al pressure tube filled with monoisopropyldiphenyl ($C_{15}H_{16}$). Such substitution was determined to be adequate by calculation. The pattern of the substitution, with the location of the measuring element, is shown in Fig. 1.

The fuel element studied was the version for physics measurements of the clustered element ESSOR C-2 foreseen for the first charge of ESSOR, a material testing reactor under construction at the CCR EURATOM Ispra. This version, named ESSOR C-2 ϕ , consists of 4 Al-clad UC rods, 25.2 mm in diameter, inserted in a graphite matrix in turn contained inside a 91 mm dia. Al tube. Between each fuel rod and the graphite matrix exists a 2.5 mm thick annular void along which circulates the organic coolant (Termip, $C_{10}H_7CH_3$). The graphite matrix is supported by a stainless steel tube (dia. 6.4/10.4 mm) on the cluster axis. The details of the ESSOR C-2 ϕ element geometry are shown in Fig.2.

Due to manufacturing difficulties, the element designed for this experiment differed in some detail from the ESSOR C-2 ϕ element. In particular, the lack of impermeable graphite required the addition of a 0.5 mm thick Al tube to contain the organic liquid (Diphyl instead of Termip). Clearly these differences do not have any effect on the experimental results. In Fig.3 are shown the details of the geometry of such a modified element which, for convenience, in the present work is referred to as "ESSOR Standard".

Two modified versions of such element, representing increasing degrees of fuel poisoning (mook-up of the progressive burn-up of the ESSOR core) were realized, by filling the cluster central steel tube by either a 6.2 mm thick stainless steel rod ($\sum_a = 0.210 \text{ cm}^{-1}$) or a 6.2 mm thick nickel rod ($\sum_a = 0.430 \text{ cm}^{-1}$).

A third version of the basic element was obtained by replacing the central steel tube by a 10 mm dia. Al rod. Such version was representative of an hypothetical ORGEL-type power reactor fuel element of the same geometry as the ESSOR C2 ψ . This element was investigated with and without the organic liquid around the individual rods of the cluster, in order to provide data useful for a test of both the basic cross sections used for the organic coolant and the calculation methods employed for the determination of the hyperfine structure of the thermal flux in such type of elements. The main characteristics of the five configurations investigated are presented in Table 1.

The element fabricated for the experiment was 1 m long, the four rods being kept fixed with the proper geometry by two stainless steel end-plates. Two opposing rods of the element were specially designed to contain the detectors of the thermal flux distribution, and consisted each of three 30 cm long (in UC) segments, rigidly connected. The central rod-segment was an assembly of precision machined UC pellets, sliding inside an Al tube provided with removable end-caps (leak-proof). The central UC pellet had a series of small cavities where the detectors were contained. A minor (less than 0.15 mm) clearance existed between the UC rod and the Al canning. Details of this fuel element and of the measuring rods are given in Fig.4 to 7.

The thermal flux detectors were 2 mm dia., 0.20 mm thick disks made from a high purity Dy-Al alloy, containing 10% of Dy by weight. Six sets of about 40 detectors each were used; the intercalibration factors of the detectors of each set were obtained by four successive irradiations in a uniform flux.

In the set were included only those detectors whose inter-calibration factors resulted determined with an uncertainty of less than 0.5% (defined as the mean square deviation from the mean of the values obtained from the four independent irradiations), and differed from the average value for the set by less than +1%. The last condition assured that even in case of confusion among the detectors (which could not be marked, due to their small size) the uncertainty introduced in the experimental data would not exceed +1%.

The detectors were arranged in the measuring rods in concentric rings, both inside the fuel and on the surface of the Al tubes, as indicated in Fig. 8 and 9. In particular, the detectors in the fuel were positioned inside 2.1 mm dia., 0.4 mm deep cavities, precision-machined (by the electroerosion technique) on the flat face (horizontal position) and on the curved side (vertical position) of 2.5 cm high UC pellets. These pellets were arranged in the measuring rods so that the horizontal detectors were placed at the mid-plane of the 1 m long element. At such position the effect of the thermal flux peaking produced by the end-caps of the central rod-segment was negligible, as shown also in previous experiments (5).

The detectors on the surface of the Al tubes (i.e. rod claddings and pressure tubes) were fixed vertically by an adhesive mylar tape, about 0.005 mm thick, at the same height as the detectors in the fuel. The detectors inside the fuel were sandwiched between two 0.03 mm thick high-purity Al disks, to prevent their contamination by fission products capture.

The distribution of the detectors on the concentric rings was made along the 3 main directions for the thermal flux variation in the cluster, i.e. along the rod radii forming with the axis through the centers of the rod and of the cluster the angles of 0° , 45° and 90° , respectively (see Fig.8).

Perturbation effects of various nature which could have been produced by the Dy-Al detectors were made negligible by proper selection of the experimental set-up. In particular, the minimum distance between adjacent detectors was determined by calculation (6) so as to make the shadow effect unimportant. The correction to be applied to the data for the different self-shielding and flux depressions, caused by the foils themselves when placed inside the fuel and on the surface of the Al tubes (these perturbations are dependent on the medium surrounding the foil), was calculated by standard methods (7) to be negligible. Similarly, it was estimated to be trivial the effect of a non isotropic flux distribution on the activation of the foils placed vertically at the boundaries of the different media in the cluster, because of the type and size of detectors used.

The contribution to the total Dy¹⁶⁴ activation from neutron capture at energies above the Cd cut-off was determined by a measurement of the Cd-ratio for Dy¹⁶⁴, using two 4 mm dia., 0.01 mm thick pure Dy detectors, one bare and one clad by cadmium, fixed to the outer surface of the Al tube containing the cluster. The thickness of the cadmium box was 0.80 mm, corresponding to an effective cut-off about 0.50 ev. The two detectors were placed at 180° , at symmetric flux positions.

The very small correction factor for the macroscopic flux variation across the clustered fuel element (as it is shown in Fig.1 the measuring element is not at the center of the lattice) was determined by activating two sets of Dy-Al foils on the cluster outer Al tube, at 180° along the direction of maximum flux gradient. On the assumption of a linear flux variation along such direction, the amount of the correction varied from zero for the data-points close to the outer boundary of the cluster to a maximum of about 1.5% for the data-points close to the center of the cluster.

Among the modifications of the experimental details of the present measurements with respect to the previous work (1,2,3), the following are worth noting.

Firstly, the Dy-Al detectors fixed to the lateral surface of the UC rods permitted the determination of the flux value at the interface UC-Al cladding, which, together with the corresponding flux value at the outer surface of the Al cladding, defined with a rather good accuracy the shape of the flux through the cladding itself.

In the previous experiments such flux point was not measured and the flux across the Al canning was inferred either by a linear extrapolation of the flux curve measured inside the fuel, or by assuming a constant flux through the thickness of the cladding. The two extreme assumptions were used for the cases of "large fuel rod diameter-thin cladding", and "small fuel rod diameter thick cladding", respectively. The justification for the choice of the assumptions is obvious.

Secondly, by arranging the detectors in complete concentric rings it was made possible to correct for accidental relative rotations of the components of the cluster during the assembly of the measuring rods (particularly of the UC pellets inside the clad). Such correction was inferred from an analysis of the plot of the detailed azimuthal flux distributions in the UC and on the Al cladding and pressure tube. Relative phase shifts of these curves could be accurately determined and corrected for. It was estimated that the error introduced in the data when applying this correction could not exceed $\pm 0.5\%$.

After the irradiation, the beta activities induced in the Dy-Al detectors were measured by means of an automatic chain of eight plastic scintillation counters. Standard corrections were applied to the data for room background, counter efficiency and dead time, efficiency and decay of detectors.

RESULTS

The results of the measurements are presented in Table 4 and Fig. 10 to 16. The data are presented as total Dy¹⁶⁴ activations, normalized to unity at the outer surface of the Al tube containing the cluster. In Table 4 are given the Dy¹⁶⁴ Cd-ratios, measured at the cluster outer boundary.

From these data and the knowledge of the spectral distribution of the neutron flux (thermal and epithermal) typical of this kind of D₂O moderated lattices, the corresponding thermal flux and/or neutron density distributions can be easily determined, using the measured parameters of the - 1.86 eV neutron resonance of Dy¹⁶⁴ (8). In fact the correction for the epi-thermal activation of Dy is not important, being in any case smaller than the experimental error, as it may be shown by elementary considerations.

For convenience, in the following part of the report the total Dy^{164} activation distributions will be referred to as thermal flux distributions.

The radial thermal flux distributions measured in the five fuel element configurations considered (see Table 1), along the three main directions corresponding to $\vartheta = 0^\circ, 45^\circ$ and 90° , respectively, are shown in Fig.10 to 14. Also given in the figures are the smooth curves through the experimental points. Two typical azimuthal distributions of the flux (i.e. as a function of ϑ , with constant r) are presented in Fig.15 and 16.

The close resemblance of the flux curves measured for the three cluster configurations corresponding to increasing degrees of poisoning of the ESSOR C-2 element (see Fig.10, 11 and 12) was expected, since the absorption by the poison represents only a minor fraction of the total neutron capture in the cluster and is localized in a narrow region along the cluster axis. Nevertheless it was considered worthwhile to perform the measurements for the three cases, because the experimental technique was enough accurate to put in evidence even minor differences in the flux distributions.

The important effect of the organic coolant on the hyperfine structure of the thermal flux is shown by the comparison of Fig.13 and 14.

The measured flux variation across the Al cladding of the fuel rods has verified the assumption made previously (3), that an adequate representation for the flux across the thin Al cladding of a large fuel rod can be obtained by a linear extrapolation of the flux curve measured inside the fuel.

The most likely experimental errors were caused to occur at random in successive measurements, by a careful determination of the details of the experimental procedure. Thus were random errors those deriving from the uncertainties in detector efficiency, radial and azimuthal position of detectors, measured counting rates of the detectors (from counting statistics, counting equipment drifts, variation in detector-to-counter spacing), etc.

The contribution of such random errors is included in the quoted experimental uncertainties, defined as the standard deviations of the means of the results of sets of 4 independent measurements.

The remaining sources of error, which were systematic to the above sets of measurements (such as those deriving from local flux perturbations and screening effects caused by the detectors themselves, etc.), were estimated not to give a significant contribution to the overall uncertainty of the data.

It was concluded that the error estimate obtained from the spread in the experimental results was a reasonable evaluation of the total errors involved in the measurement. These errors were typically +1%.

The semi-empirical analytical expression, which was found to describe with very close approximation the measured thermal flux distributions in similar UC clustered fuel elements (3), was tested against the results of the present experiment. Such expression is :

$$\phi(r, \vartheta) = p e^{\xi r^2} + q \sqrt{\frac{r}{R}} \cos \vartheta e^{\xi r} \quad (1)$$

where : r, ϑ are the polar coordinates referred to the center of the fuel rod (see Fig.8), R is the distance from the center of the cluster, p, q, ξ are experimentally adjusted parameters.

The practical usefulness of Eq.1 (provided it can reproduce the measured flux distributions with adequate accuracy in a wide range of cluster configurations) stems from the fact that it allows the determination of the detailed hyperfine structure distribution in clustered elements of complex geometry, from data taken at few readily accessible points in the elements. It is reminded that at present there is no simple way of calculating with close approximation the detailed hyperfine structure of the thermal flux in clustered fuel elements.

The reproduction of the measured flux distribution was found to be somewhat improved by using two different values of q in Eq.1, for $\cos \vartheta \geq 0$. Similarly to what noticed in the previous work (2, 3, 9), the value of ξ was found to vary only slightly for the five cluster configurations considered, so that a satisfactory fit was obtained using for all cases the average value of ξ .

The analytical curves describing the measured hyperfine structure of the five cluster configurations investigated are shown in Fig.17 to 21. The values of the parameters p , ξ , q_1 (for $\cos\mathcal{D}=0$) and q_2 (for $\cos\mathcal{D}\neq 0$) utilized, are shown in Table 3. The experimental and analytical flux distributions are compared, for a typical case, in Fig.22 to 24 (radial flux distributions for $\mathcal{D} = 90^\circ, 45^\circ$ and 0° , respectively). Except for one or two data-points, the agreement is within the limits of the overall error quoted for the experiments (normally $\pm 1\%$, $\pm 3\%$ in the case of the 19 rods U cluster).

With the good result of the present test, the practical interest of expressions of the type of Eq.1 (the original expression proposed by P. Palmedo (9) for gas cooled, D_2O moderated, UO_2 clusters, was :

$$\phi_i(r, \mathcal{D}) = (p_i + q_i r \cos \mathcal{D}) e^{-\xi_i r^2}$$

where the index i refers to the representative rods of the cluster) in describing the hyperfine distribution of the thermal flux in clustered fuel elements of complex geometry, may be considered to be definitively proved.

The main characteristics of the fuel elements for which a comparison between measured and analytical flux distribution has been made are shown in Table 3; it appears that the range of validity of such analytical representation is remarkably wide.

In all cases the agreement is (except for very few data-points) better than the quoted experimental accuracy; since in most cases the experimental error was $\pm 1\%$ or less, there is an indication that the accuracy of the analytical description of the hyperfine structure of the thermal flux is about $\pm 1\%$. This accuracy is largely sufficient for thermodynamics, mechanical deformation and most reactor core physics studies.

The reduction in the amount of experimentation needed to completely specify the hyperfine structure of the flux in a given clustered fuel element when Eq.1 is used, with the parameters p, ξ, q adjusted to the experiment, is substantial.

In particular, p may be determined from the flux value at the fuel rod center; ξ, q_1 and q_2 from flux values on the outer surface of the rod cladding at $\vartheta = \frac{\pi}{2}, \vartheta = 0$ and $\vartheta = \pi$, respectively. Then only one flux-point must be measured inside the fuel rod (on the rod axis, where an exact positioning of the detector is unimportant) and the experimental set-up can be considerably simpler than the one used for the present work.

Besides
Besides, the parameter ξ determined from the fit to the flux distribution measured in a cluster, can be often extrapolated to related cluster configurations; in this case the remaining parameters p, q_1 and q_2 are defined from flux point-values measured on the outer surface of the cladding of the representative rods of the cluster considered, and there is no need to measure the flux inside the fuel rod.

AKNOWLEDGMENTS

The authors are indebted to Mr. S.TASSAN for his continuous support and useful criticism, to Mr. A.BOEUF for helpful discussion and advice, to Mr. L.HAEMERS for his determining technical assistance, to Messrs. C.LANDES and C.DUMONT for the fabrication of the UC clustered fuel elements used for the experiment, to Mr. V.RUGGERI for the intercalibration of the Dy detectors, to the personnel of the AQUILON II critical facility at CEN Saclay (and particularly to Messrs. FRICHET, ZAMITTE and PAVRET DE LA ROCHE FORDIERE). They wish to thank Mr. A.CARETTA for the drawing of the figures contained in the report.

REFERENCES

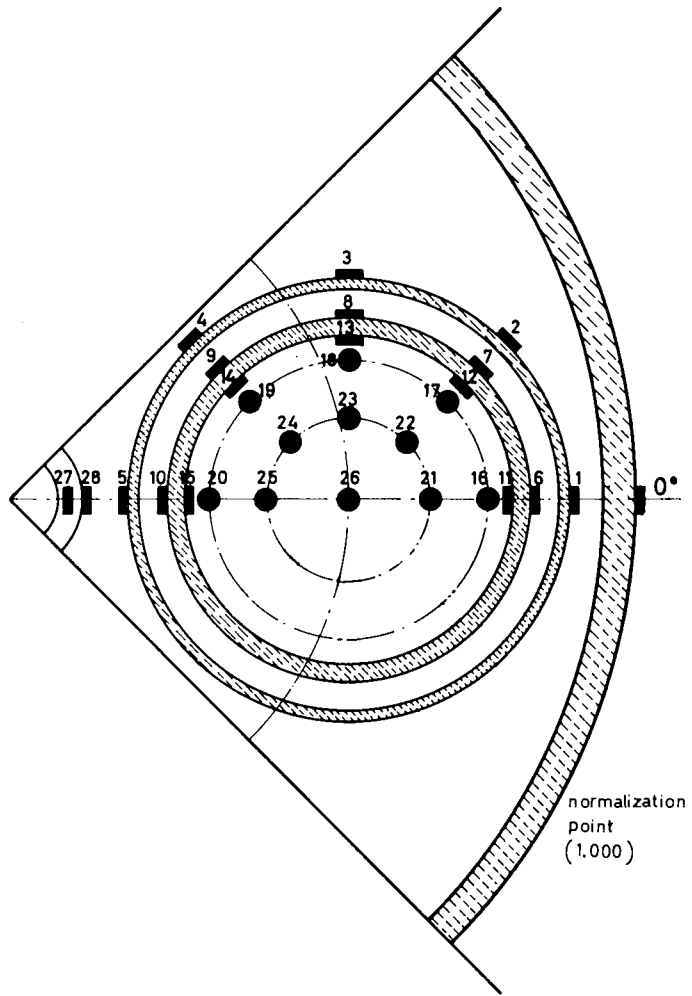
- (1) A.Boeuf, S.Tassan
A measurement of the fine structure of the thermal flux in simple geometry ORGEL type lattices. EUR 206e
 - (2) A.Boeuf, S.Tassan
A measurement of the fine structure distribution of the thermal flux in organic cooled fuel elements in a D_2O moderated lattice. *Energia Nucleare*, 11, 10, 533 (1964)
 - (3) A.Boeuf, S.Tassan
A measurement of the hyperfine structure of the thermal flux distribution in organic cooled UC clustered fuel elements in a D_2O moderated lattice. Submitted for publication to *Energia Nucleare*.
 - (4) Y.Girard, et al.
Proc. Second Geneva Conference on Peaceful Uses of Atomic Energy, 12, 281 (1959)
 - (5) A.Boeuf, S.Tassan
Personal communication
 - (6) M.Reier, J.A.De Juren
Reactor Sci. and Tech., 14, 1 (1961)
 - (7) C.W.Tittle
Nucleonics, 8, 6, 5; 9, 1, 60 (1951)
 - (8) R.Sher, S.Tassan, E.Weinstock, A.Hellsten
Nu. Sci. and Eng., 11, 4 (1961)
 - (9) P.F.Palmedo
Etudes Expérimentales de structure fine à l'intérieur des grappes d' UO_2 . Rapport SEC 131, Rapport CEA 2387 (1964), *N.S.E.*, 21, 4, 578 (1965).
-

cluster configurations	fuel	diameter of rods (mm)	number of rods in the cluster	spacing between rods centers (mm)	rod cladding (Al) (mm)		pressure tube (Al) (mm)		calandra tube (Al) (mm)		central support of graphite matrix (mm)		poison filling central support		coolant	
					ϕ_{int}	ϕ_{ext}	ϕ_{int}	ϕ_{ext}	ϕ_{int}	ϕ_{ext}	ϕ_{int}	ϕ_{ext}	material	material		ϕ (mm)
ESSOR C2 STANDARD	UC	25,2	4	37,75	25,5	27,5	32,5	34,5	91	95	6,2	10,2	stainless steel	air	--	diphyl
ESSOR C2 steel poisoned	UC	"	"	"	"	"	"	"	"	"	"	"	"	stainless steel	6,2	"
ESSOR C2 nickel poisoned	UC	"	"	"	"	"	"	"	"	"	"	"	"	nickel	"	"
ORGEL version	UC	"	"	"	"	"	"	"	"	"	rod	10	aluminum	---	---	"
ORGEL version without coolant	UC	"	"	"	"	"	"	"	"	"	"	"	"	---	---	air

Table 1: Details of all investigated configurations

TABLE 2
EXPERIMENTAL RESULTS

DETECTOR POSITION	ESSOR C2 (STANDARD)	ESSOR C2 (STEEL POISONED)	ESSOR C2 (NICKEL POISONED)	ORGEL VERSION OF ESSOR C2 (STANDARD)	ORGEL VERSION OF ESSOR C2 (WITHOUT ORGANIC COOLANT)
1	.946 1.1%	.936 0.9%	.943 0.3%	.959 0.3%	.917 0.3%
2	.888 1%	.888 1.3%	.901 0.7%	.906 0.2%	.878 0.3%
3	.789 1.9%	.796 1.5%	.809 0.9%	.804 1.7%	.804 1.2%
4	.610 1.6%	.631 2%	.608 0.4%	.637 2.5%	.706 1%
5	.513 0.5%	.540 1.2%	.522 1%	.569 0.5%	.670 0.4%
6	.726 1.2%	.761 0.9%	.754 1%	.755 1.4%	.872 1.1%
7	.707 1.2%	.741 0.6%	.737 0.6%	.742 1%	.851 0.5%
8	.637 1%	.675 0.5%	.669 0.6%	.676 1%	.766 1.1%
9	.547 1.5%	.573 1.3%	.561 1.3%	.577 0.5%	.677 0.6%
10	.502 1.3%	.526 1.1%	.516 1%	.543 1%	.646 0.8%
11	.685 0.9%	.716 1%	.709 1%	.718 0.6%	.824 0.4%
12	.664 0.9%	.698 1.7%	.695 1%	.698 1%	.798 0.4%
13	.603 1.8%	.631 1%	.634 1.3%	.636 0.9%	.726 1.2%
14	.521 1.9%	.546 0.5%	.548 2%	.564 1%	.639 1%
15	.492 1.4%	.511 0	.503 1%	.530 1.2%	.609 0.5%
16	.637 1.4%	.673 1%	.663 1.3%	.668 1%	.760 1%
17	.621 1.2%	.655 1.5%	.649 1.2%	.650 1.3%	.742 1%
18	.568 1.6%	.593 0.4%	.581 0.7%	.601 1.2%	.673 0.8%
19	.498 1%	.519 0.5%	.510 0.9%	.535 0.8%	.608 0.5%
20	.473 1.3%	.493 0.9%	.485 1%	.506 0.7%	.590 0.5%
21	.552 1.2%	.579 0.5%	.577 1%	.580 0.7%	.651 0.5%
22	.540 0.8%	.563 0.7%	.558 0.7%	.570 0.4%	.640 0.7%
23	.506 1.2%	.532 0.9%	.526 1%	.536 0.6%	.607 1%
24	.473 1%	.498 1.0%	.489 1%	.507 0.4%	.570 0.5%
25	.460 1.5%	.485 0.8%	.480 1%	.496 0.6%	.564 0.3%
26	.490 0.9%	.513 0.8%	.506 0.9%	.515 0.7%	.585 0.6%
27	.500 1.2%	.467 0	.482 0.5%		
28	.510 1.4%	.520 0	.510 0	.585 0.7%	.688 1%



— VERTICAL DETECTORS
● HORIZONTAL DETECTORS

ref. (Nat. description)	fuel element	number of rods	diameter of rods (mm)	rod spacing center to center (mm)	diameter of cluster (mm)	fuel cladding	coolant type	error of measured flux points	difference between experimental analytical mean value	difference between experimental curves $\frac{N^1}{N}$	semi-empirical equations used	parameters for the equations									observations			
												P			q ₁		q ₂		ξ					
												A	B	C	B	C	B	C	A	B		C		
9	UO ₂	7	22	29	106	Ni	nitrogen	+1%	1%	2%	1/8	$\phi_1(r) = [R_1 + q_1 r \cos \theta] \xi_1 r^2$	1.000	1.103	-	0.0965	-	-	-	0.0980	0.0980	-	-	
9	UO ₂	19	12	17	106	Ni	nitrogen	+1%	1%	1%	0	$\phi_1(r) = [R_1 + q_1 r \cos \theta] \xi_1 r^2$	1.000	1.024	1.114	0.045	0.123	-	-	0.229	0.198	0.190	-	
2	U	19	12	13	81.6	Al	C ₁₅ H ₁₆	+3%	1.5%	3%	4/12	$\phi_1(r) = [R_1 + q_1 r \cos \theta] \xi_1 r^2$	0.510	0.617	0.975	0.103	0.357	-	-	0.538	0.538	0.538	-	
3	UC	4	30.9	34.7	110	Al	diphyl	+1%	0.5%	2%	1/11	$\phi(r) = [p \xi_1 r^2 + q_1 \frac{r}{R} \cos \theta \xi_1 r]$	-	0.437	-	0.106	-	0.0856	-	-	0.125	-	-	with graphite matrix
3	UC	4	30.9	34.7	110	Al	diphyl	+1%	0.5%	2%	1/11		-	0.477	-	0.0797	-	0.0868	-	-	0.130	-	without " "	
3	UC	4	30.9	30.9	110	Al	diphyl	+1%	0.5%	2%	1/11		-	0.465	-	0.0909	-	0.0933	-	-	0.1315	-	" " "	
3	UC	4	30.9	39.9	110	Al	diphyl	+1%	0.5%	2%	1/11		-	0.499	-	0.0639	-	0.0817	-	-	0.1251	-	" " "	
3	UC	7	25.2	27.5	91.6	Al	diphyl	+1%	0.5%	2%	1/7		$\phi(r) = [p + q_1 \frac{r}{R} \cos \theta] \xi_1 r^2$	0.280	0.439	-	0.111	-	0.101	-	0.106	0.110	-	-
3	UC	7	25.2	27.5	91.6	Al	air	+1%	0.5%	2%	1/7	$\phi(r) = [p + q_1 \frac{r}{R} \cos \theta] \xi_1 r^2$	0.468	0.584	-	0.111	-	0.127	-	0.0905	0.133	-	-	
present work	UC	4	25.2	37.7	91.6	Al	diphyl	+1%	0.5%	2%	1/9	$\phi(r) = [p \xi_1 r^2 + q_1 \frac{r}{R} \cos \theta \xi_1 r]$	-	0.483	-	0.0993	-	0.0905	-	-	0.150	-	-	ESSOR standard element
	UC	4	25.2	37.7	91.6	Al	diphyl	+1%	0.5%	2%	1/9		-	0.508	-	0.109	-	0.0933	-	-	0.1455	-	steel poisoned element	
	UC	4	25.2	37.7	91.6	Al	diphyl	+1%	0.5%	2%	1/9		-	0.501	-	0.1040	-	0.094	-	-	0.150	-	nickel " "	
	UC	4	25.2	37.7	91.6	Al	diphyl	+1%	0.5%	2%	1/9		-	0.512	-	0.102	-	0.083	-	-	0.142	-	ORGEL version "	
	UC	4	25.2	37.7	91.6	Al	air	+1%	0.5%	2%	1/9		-	0.580	-	0.1289	-	0.0764	-	-	0.145	-	" " " without coolant	

Table 3 : Comparison of measured and analytical flux distributions Characteristics of fuel elements investigated and parameters of the analytical expressions.

N¹ = number of experimental data points with maximum difference

N = total number of experimental data points

q₁ = for cos θ > 0

q₂ = for cos θ < 0

A = central rod

B = rod of the 1st ring

C = rod of the 2nd ring

Fuel element	Cd-ratio [ⓧ]
ESSOR C-2 standard	176
ESSOR C-2 steel poisoned	173
ESSOR C-2 nickel poisoned	174
ORGEL version of ESSOR C-2	175
ORGEL version of ESSOR C-2 without coolant	176

ⓧ measured at the outer surface of cluster tube

Table 4 : Cd-ratios measured at the clusters outer boundary

Fig.1 - Pattern of the substitution

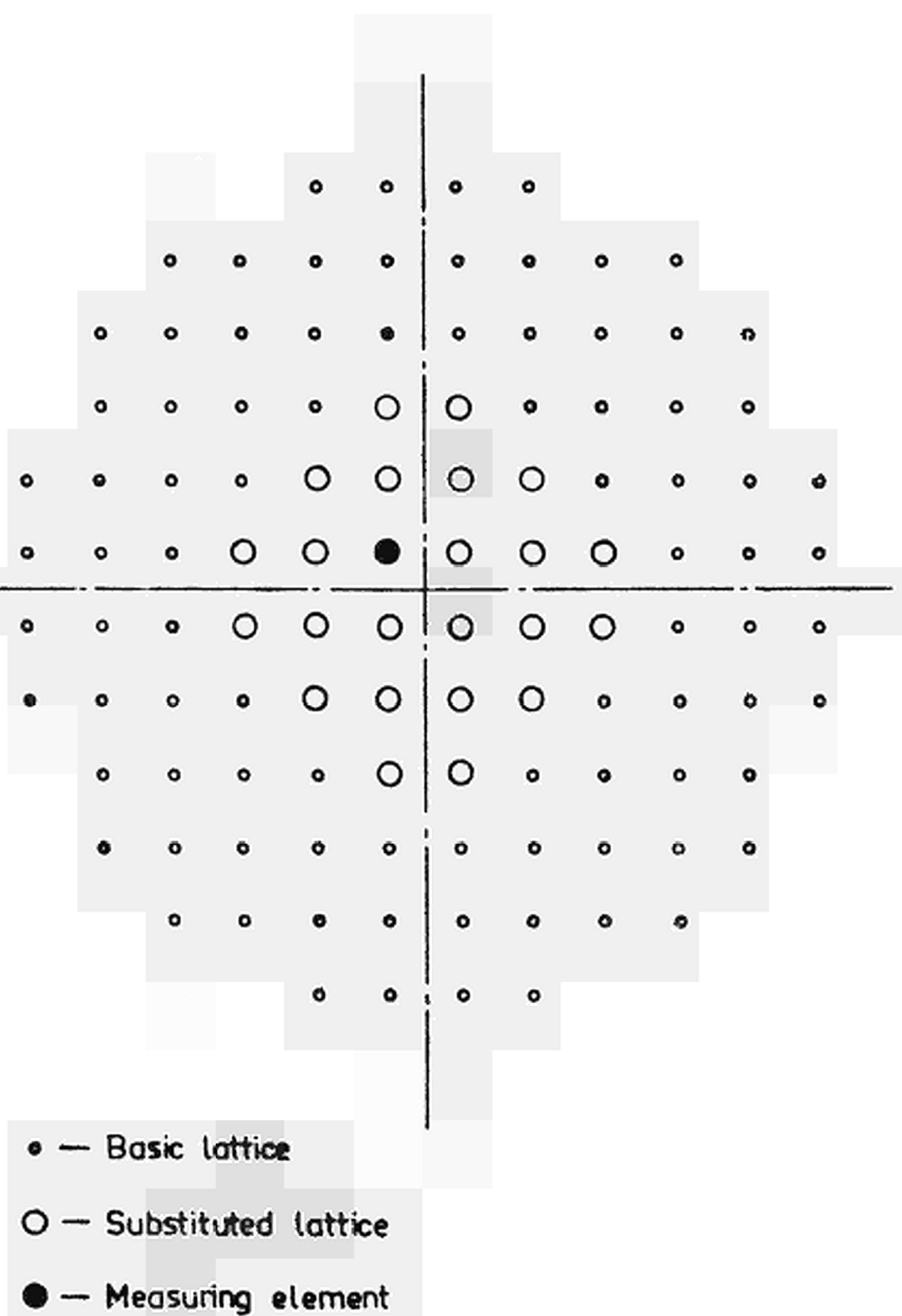


Fig. 2 GEOMETRY OF THE FUEL
ELEMENT ESSOR C2 φ

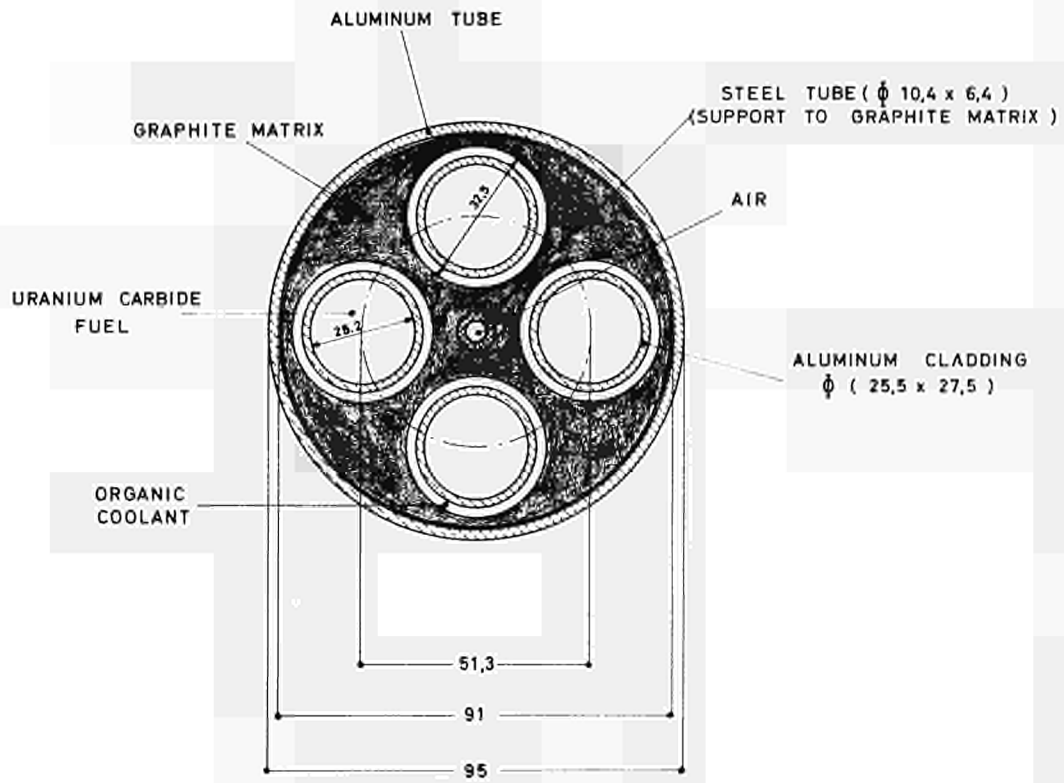
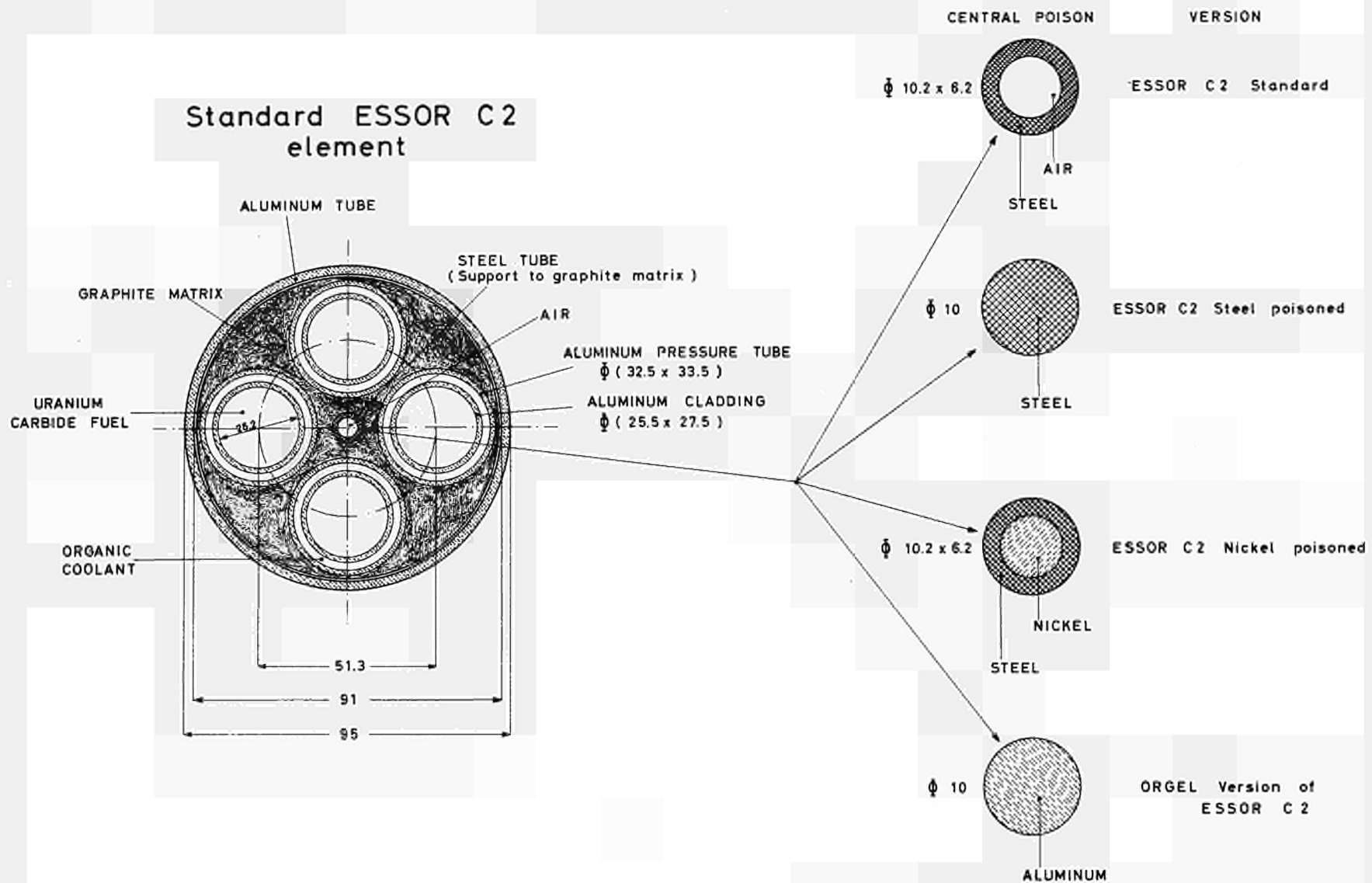
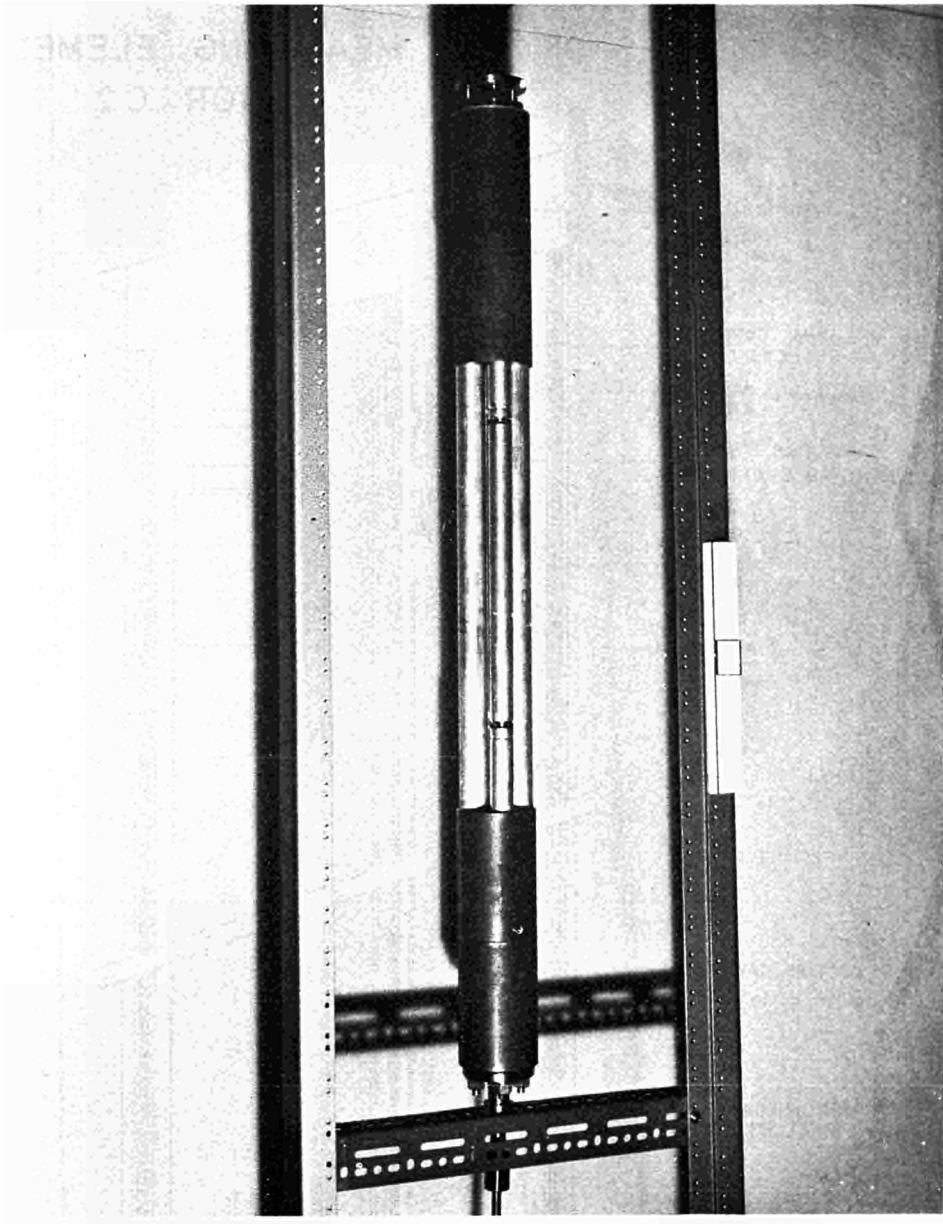


Fig. 3 GEOMETRY OF FUEL ELEMENTS INVESTIGATED

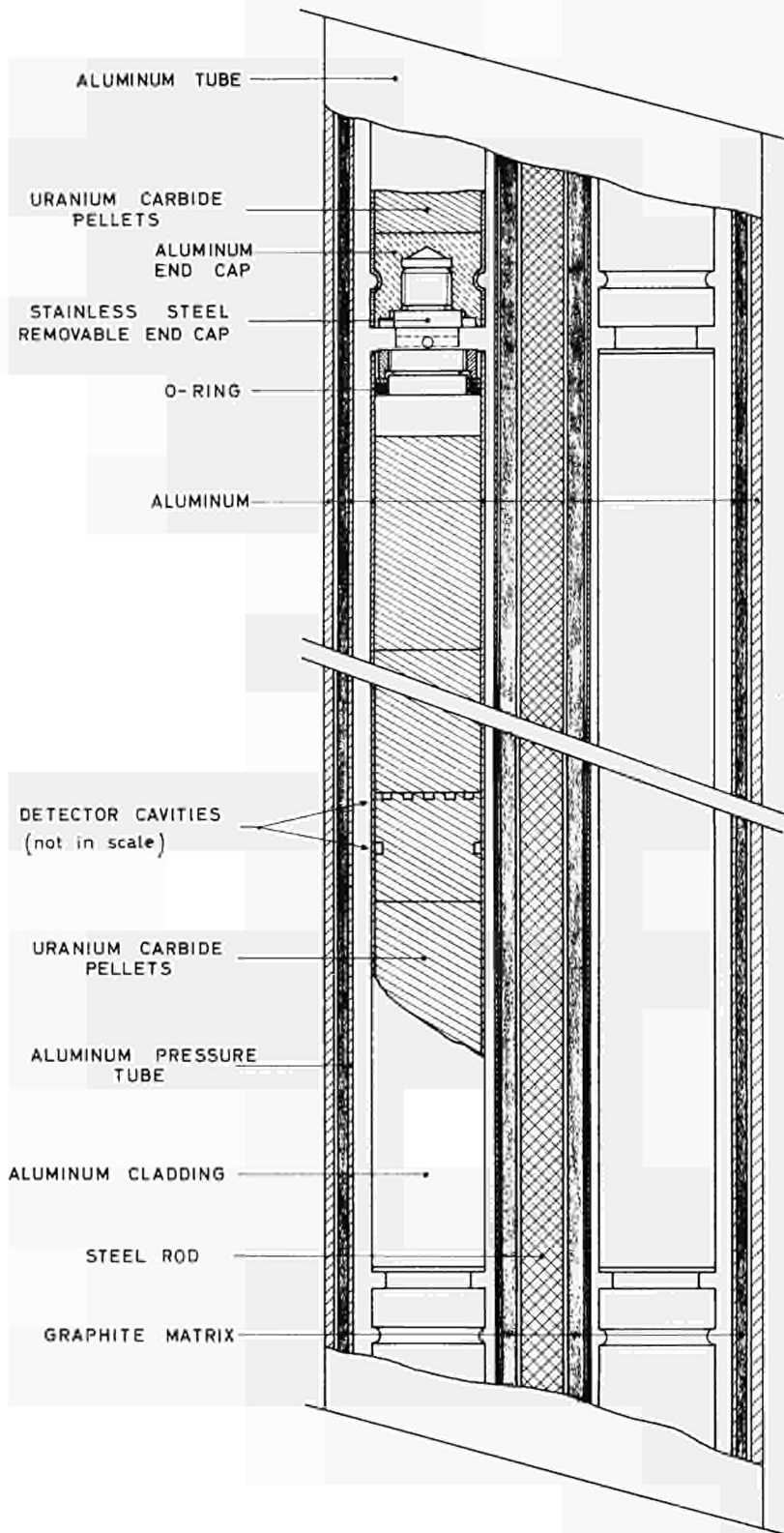


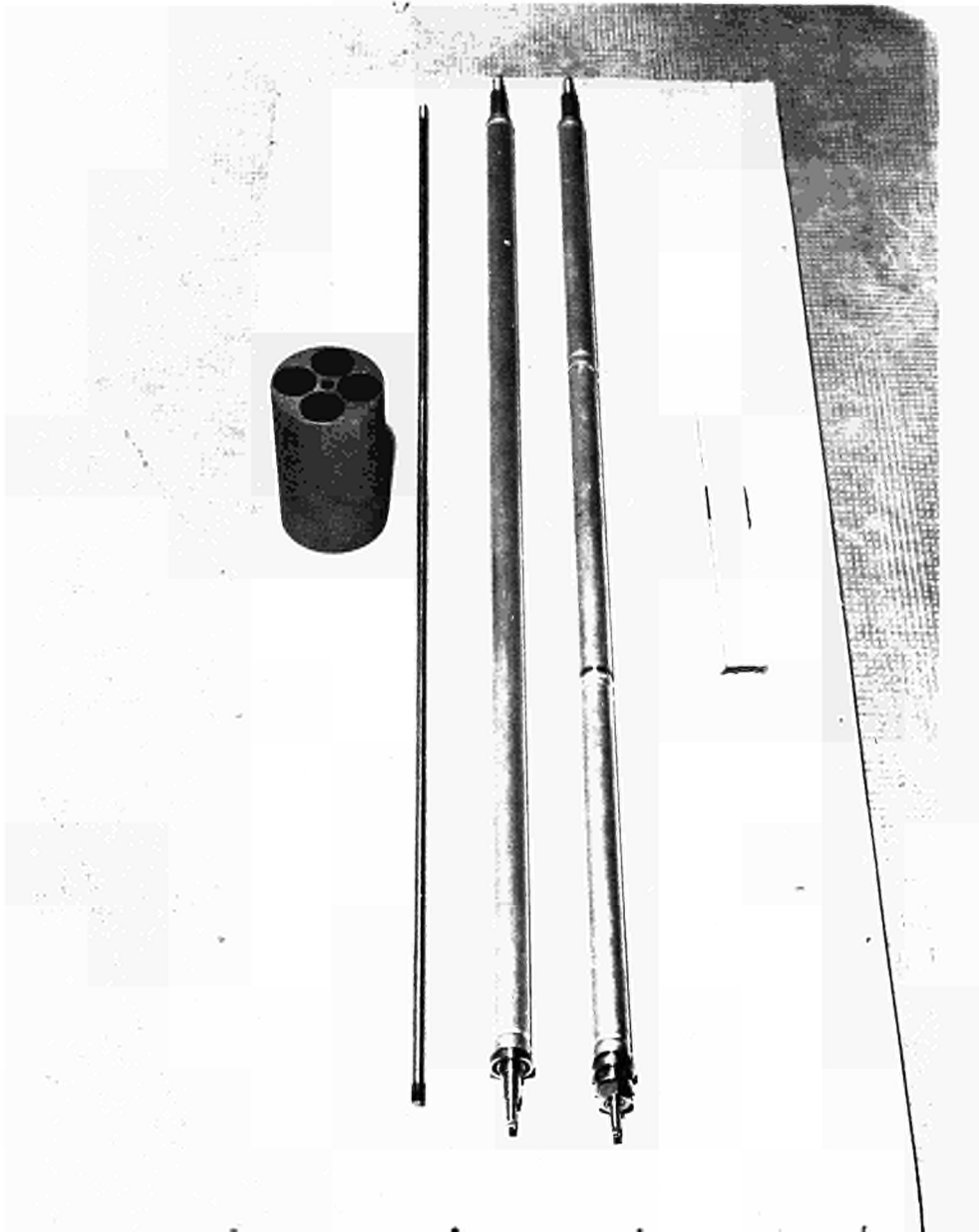


Details of the ESSOR C-2 element designed for the experiment

Fig.4 : View of the assembly with central C bloks removed

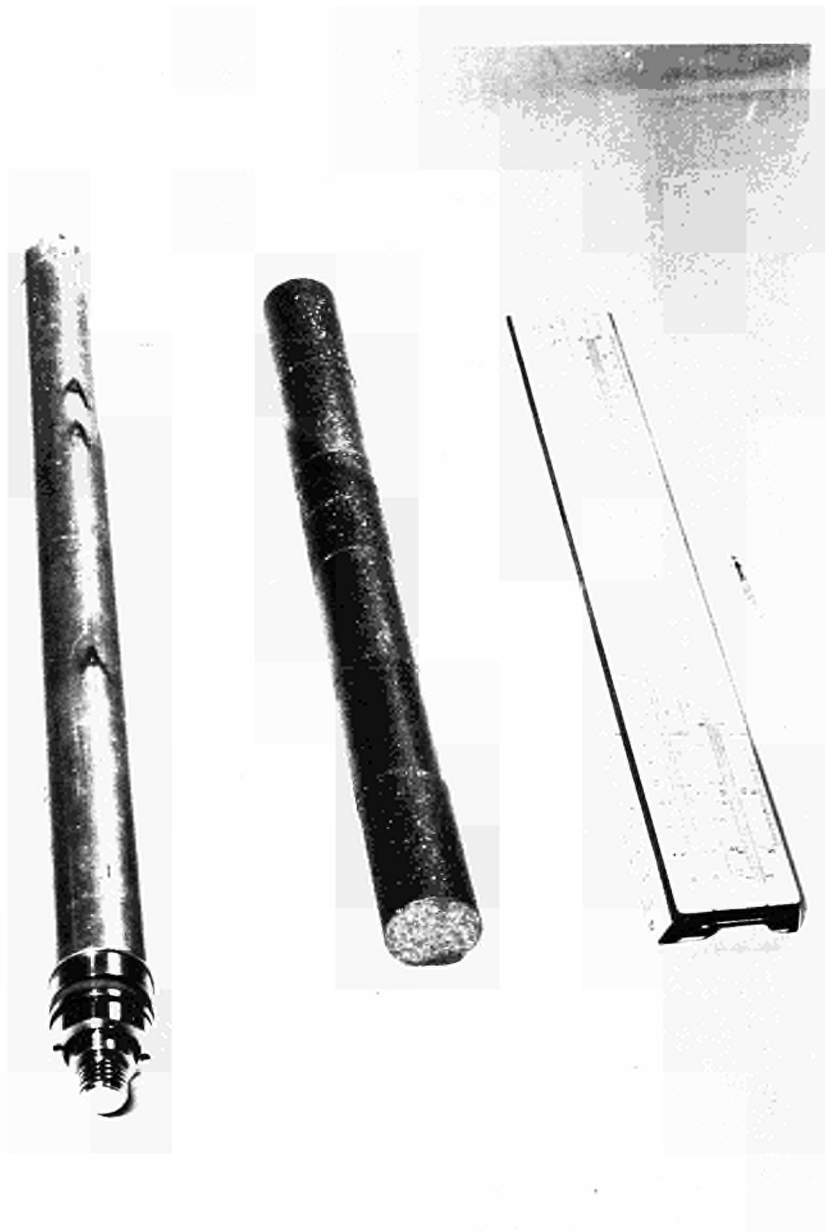
Fig. 5 DESIGN DETAILS OF THE MEASURING ELEMENT
ESSOR C 2





Details of the ESSOR C-2 element designed for the experiment

Fig.6 : Fuel rods, poison rod and graphite matrix

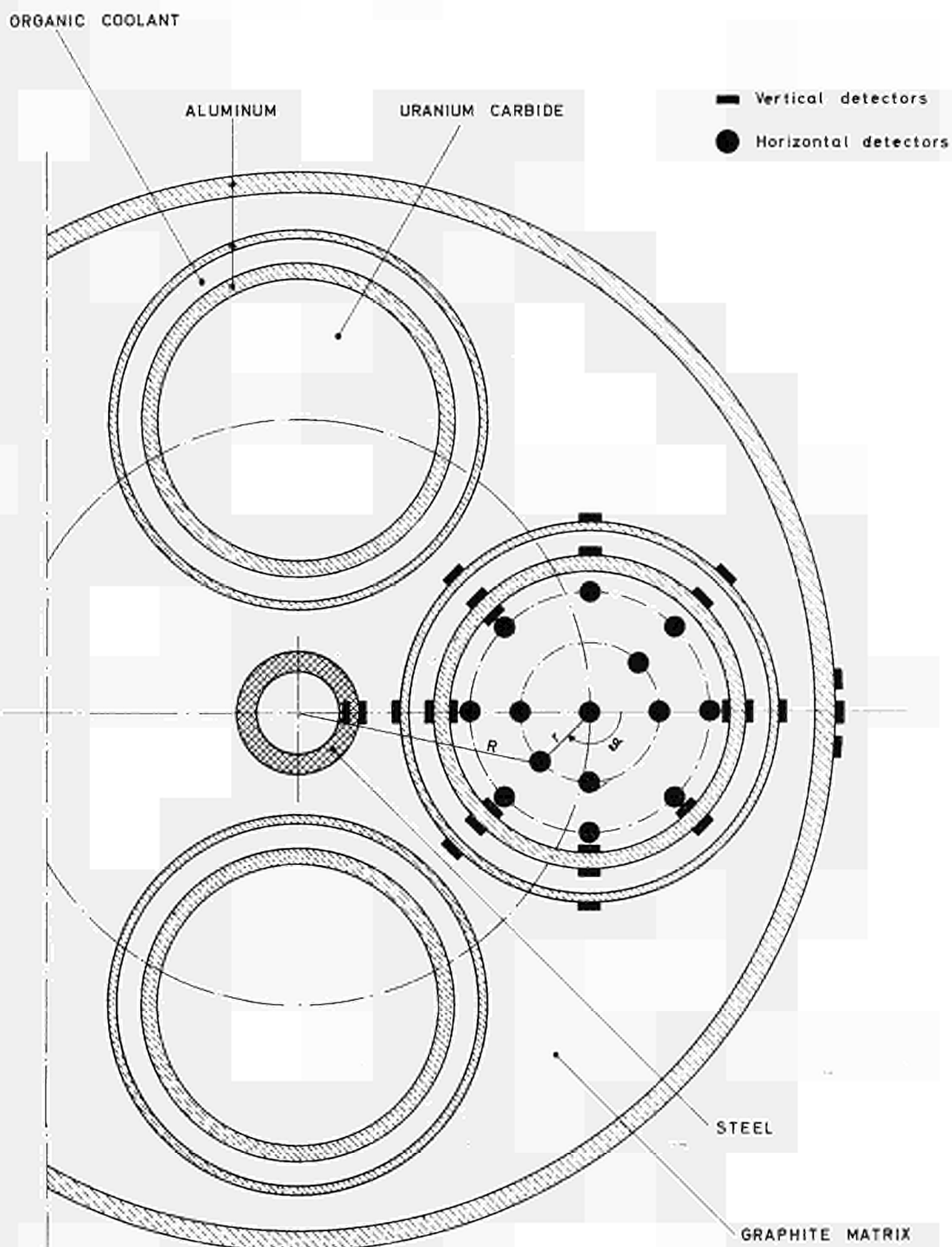


Details of the ESSOR C-2 element designed for the experiment

Fig.7 : Fuel rod segment specially designed for holding detectors

DETECTOR ARRANGEMENT IN THE MEASURING FUEL ELEMENT

Fig. 8





Details of the ESSOR C-2 element designed for the experiment

Fig.9 : UC pellet with detectors

Fig. 10 Fuel element: ESSOR C2 standard
Measured thermal flux distribution

Exp. point and curve	Flux direction
—●—	$\vartheta = 90^\circ$
—○—	$\vartheta = 45^\circ$
- - + - -	$\vartheta = 0^\circ$
—△—	$\vartheta = 0 \div 90^\circ$

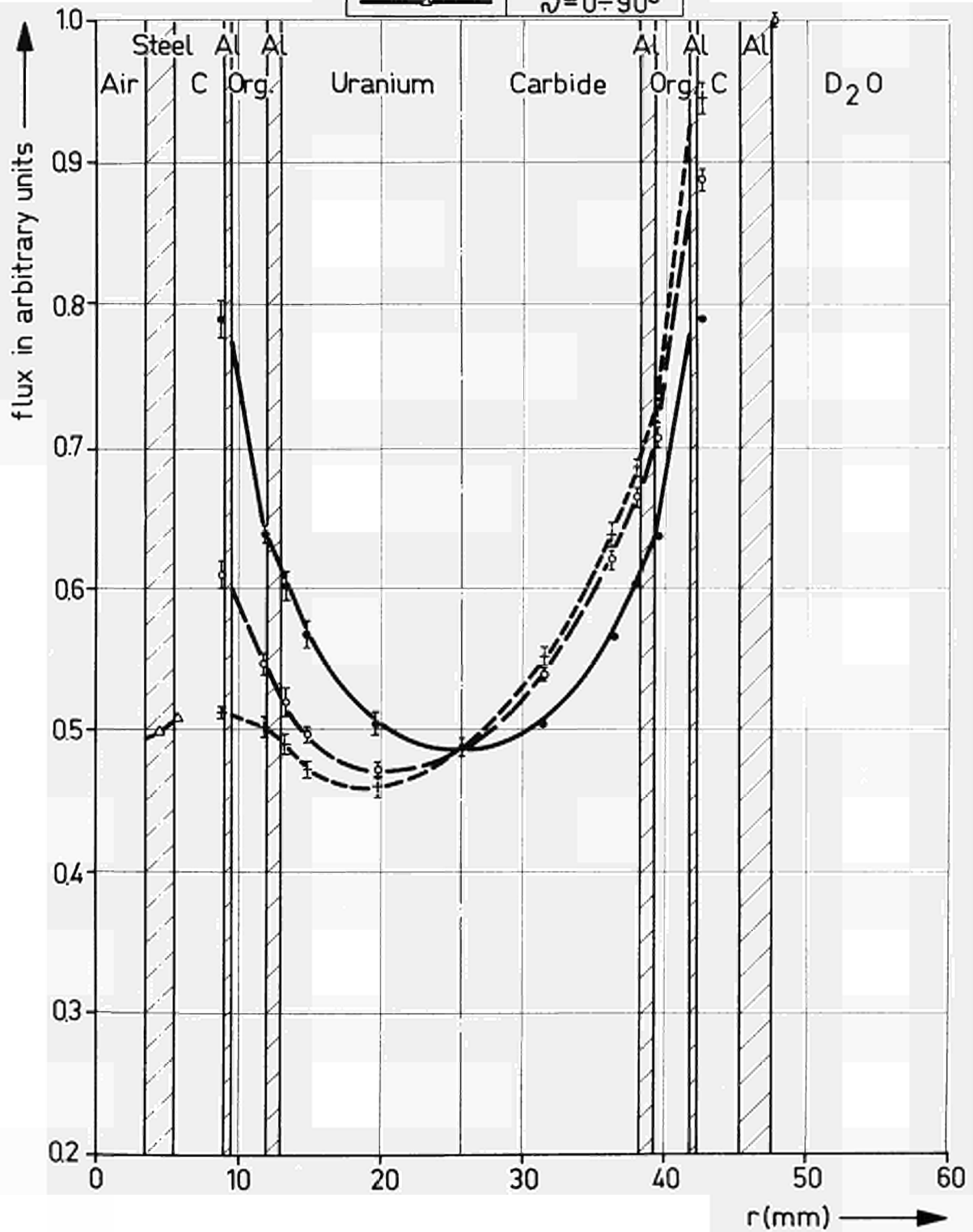


Fig.11 Fuel element:ESSOR C2 steel poisoned
Measured thermal flux distribution

Exp.point and curve	Flux direction
—●—	$\vartheta = 90^\circ$
—○—	$\vartheta = 45^\circ$
- - + - -	$\vartheta = 0^\circ$
—△—	$\vartheta = 0-90^\circ$

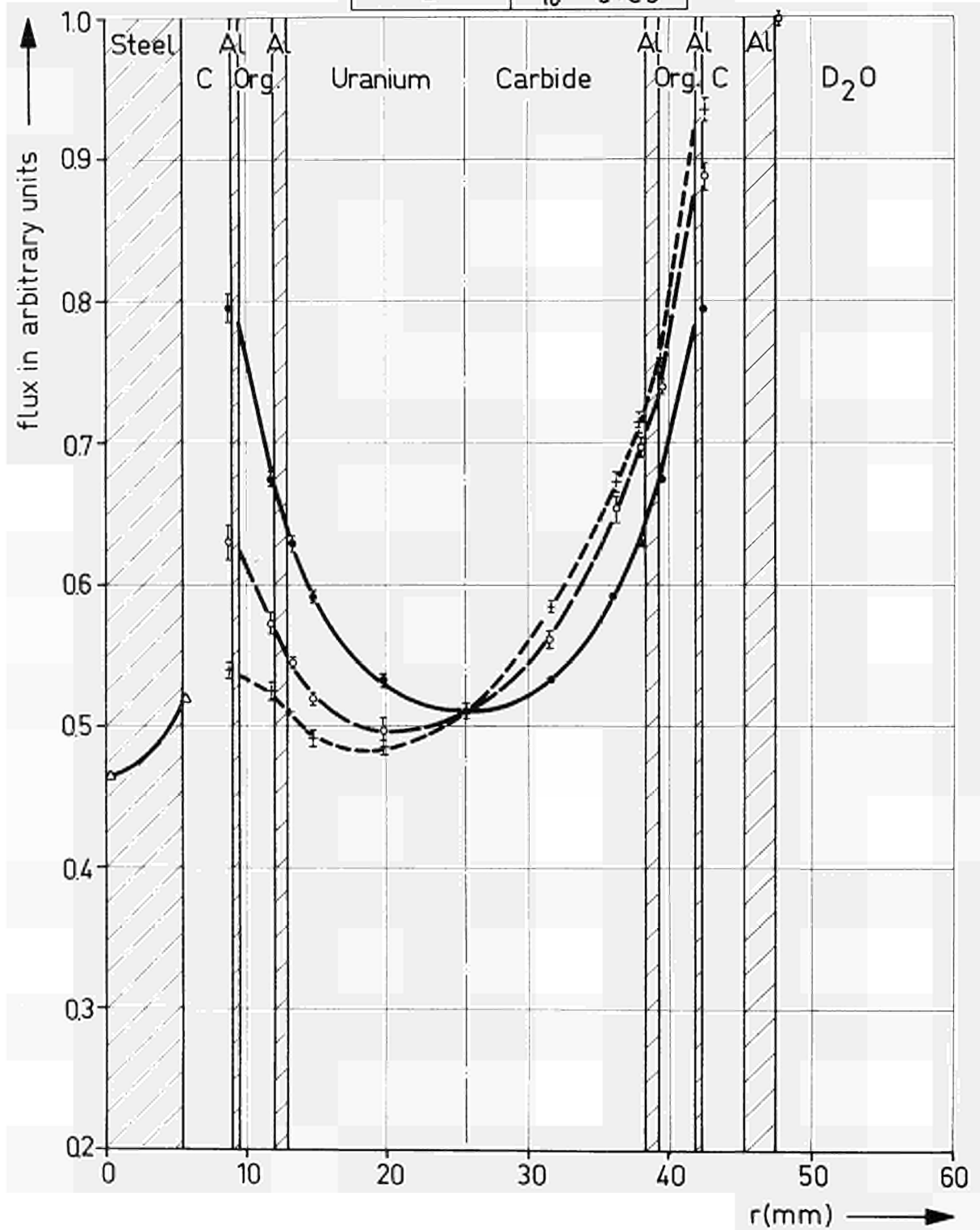


Fig.12 Fuel element:ESSOR C2 nickel poisoned
Measured thermal flux distribution

Exp. point and curve	Flux direction
—●—	$\vartheta = 90^\circ$
—○—	$\vartheta = 45^\circ$
- - + - -	$\vartheta = 0^\circ$
—△—	$\vartheta = 0 \div 90^\circ$

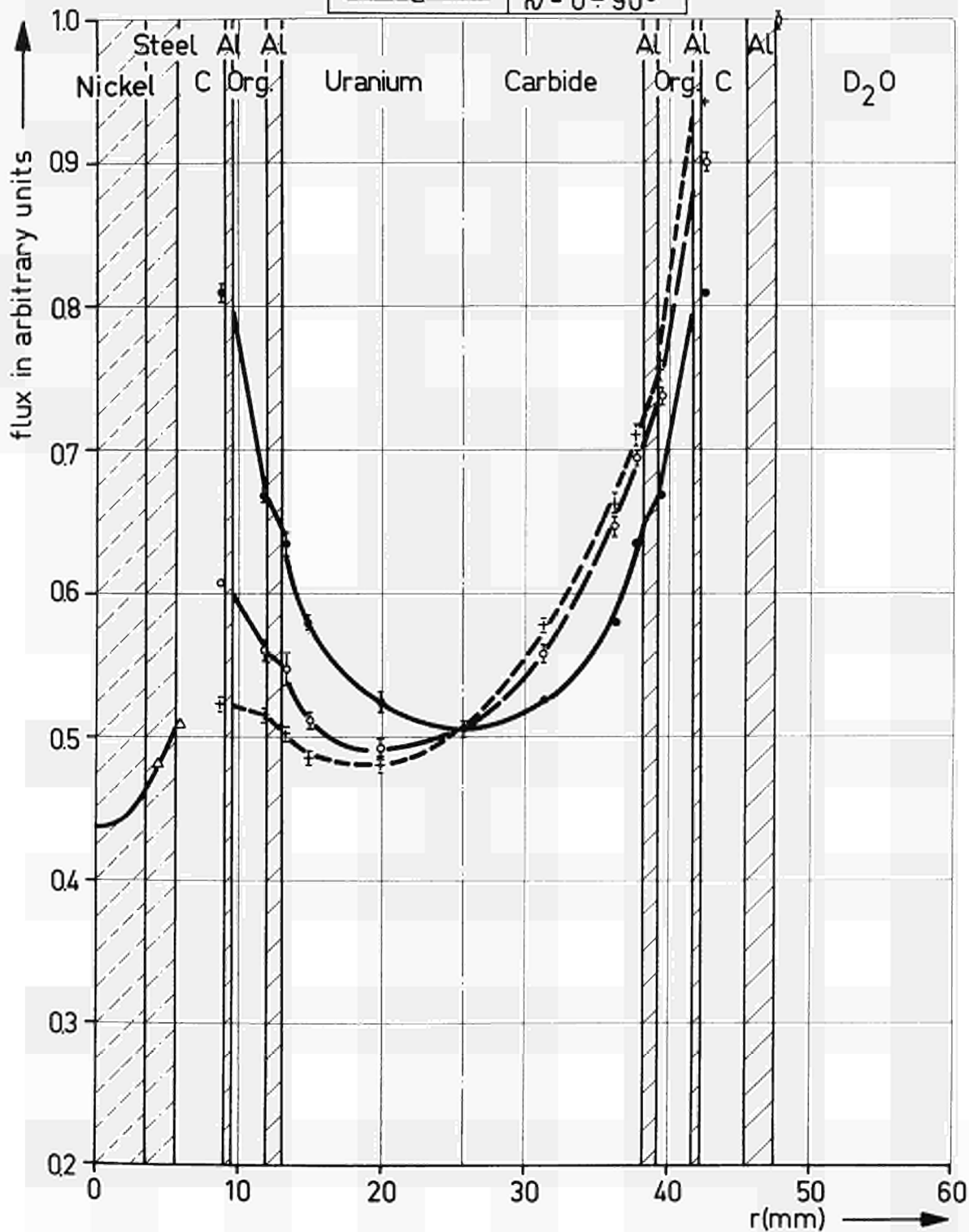


Fig.13 Fuel element:ORGEL version of ESSOR C2 with diphyl.Measured thermal flux distribution

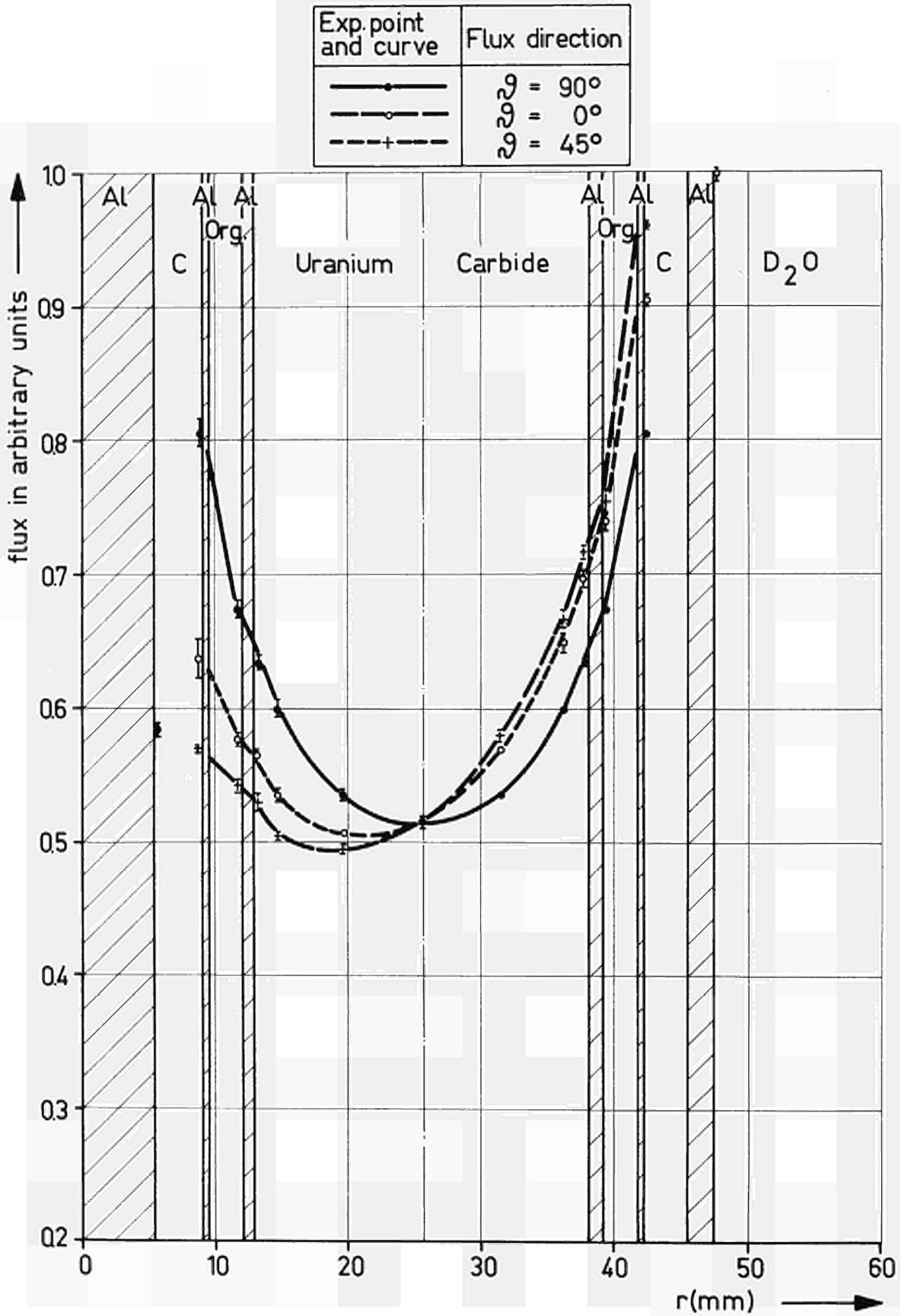


Fig. 14 Fuel element: ORGEL version of ESSOR C2 without diphyl. Measured thermal flux distribution

Exp. point and curve	Flux direction
—●—	90°
—○—	45°
—+—	0°

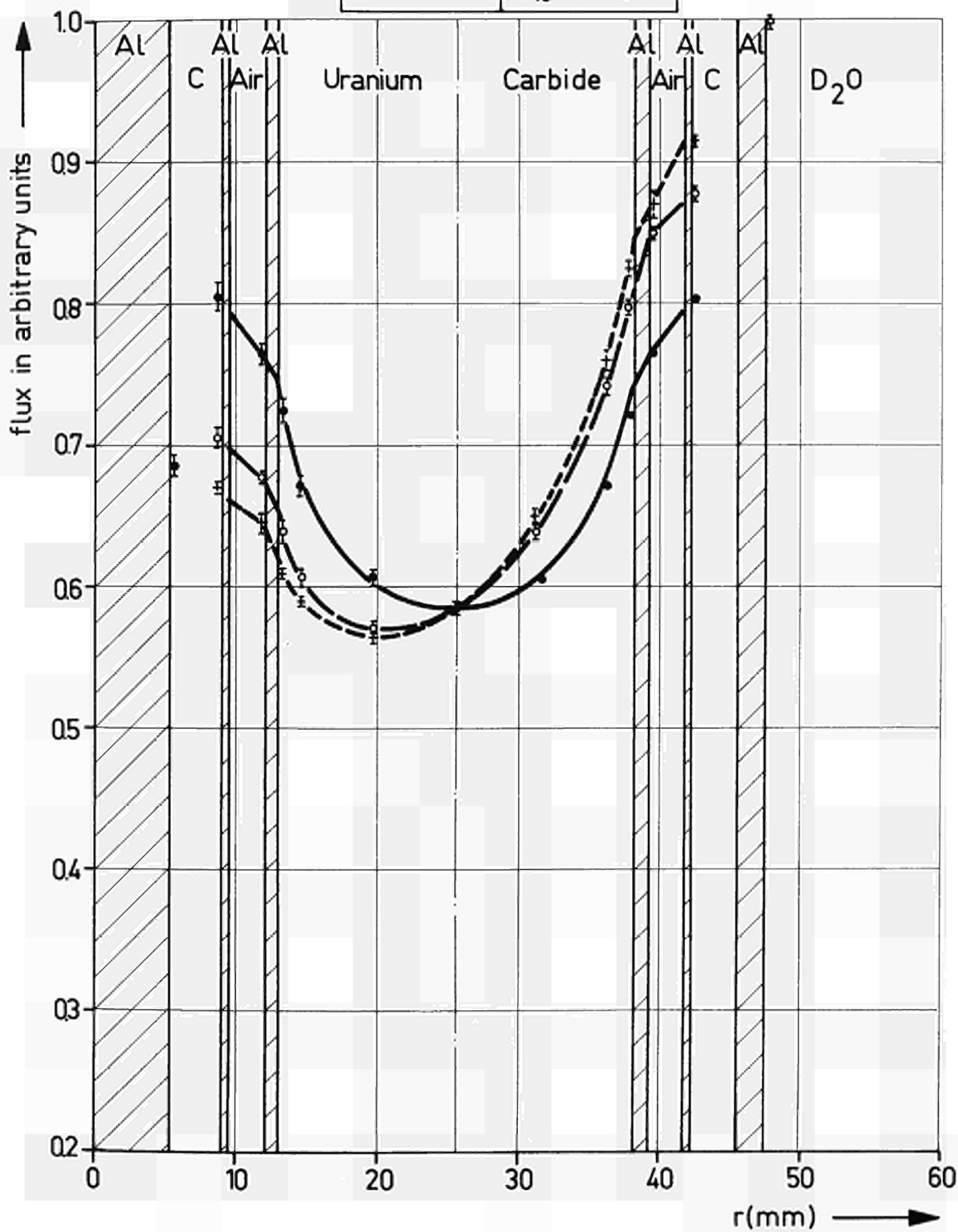


Fig.15 Detailed azimuthal distribution of the thermal flux in one rod of the ESSOR C2 standard

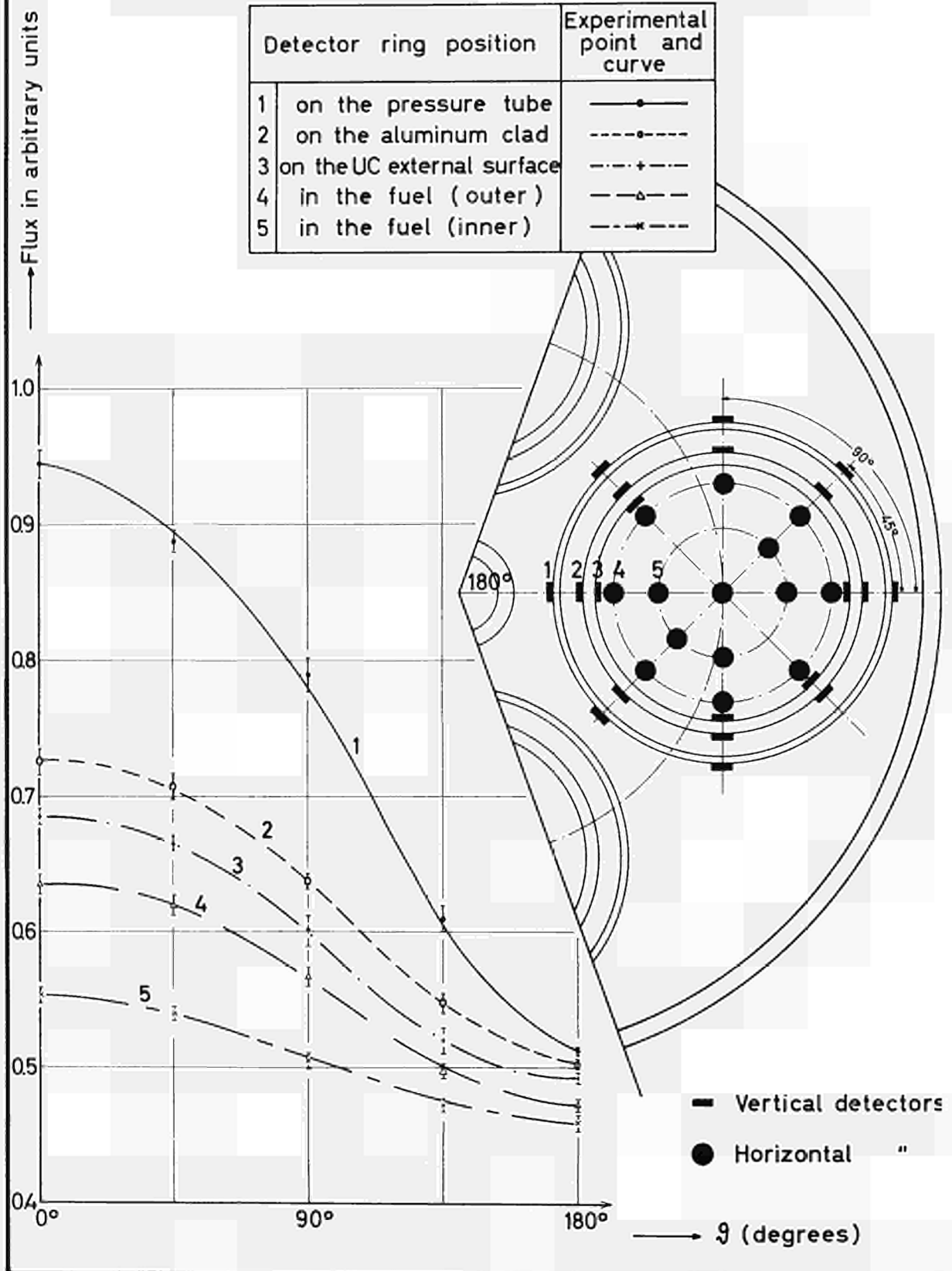


Fig. 16 Detailed azimuthal distribution of the thermal flux in one rod of ORGEL version of ESSOR C2

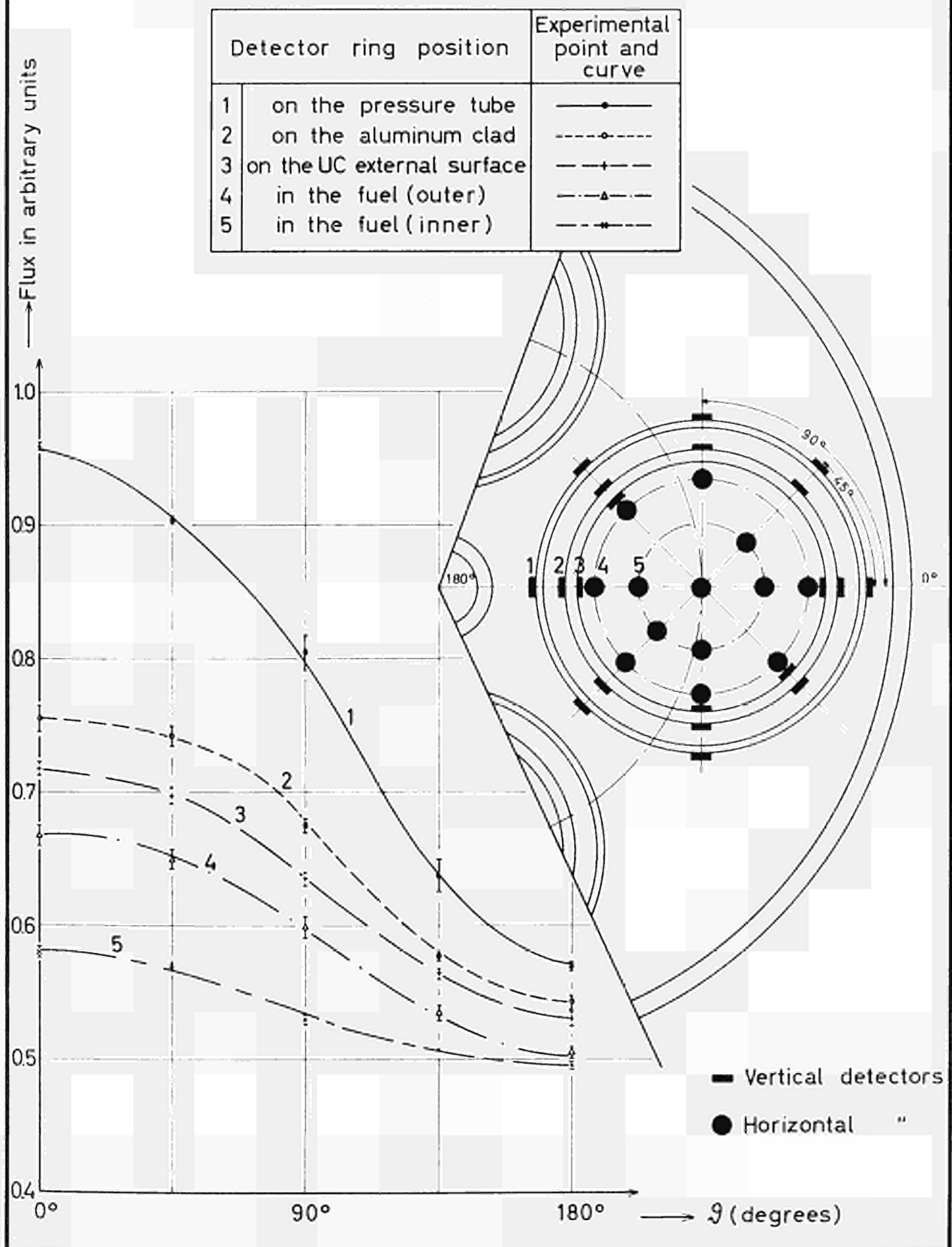


Fig.17 Fuel element:ESSOR C2 standard
Analytical thermal flux distribution

Exp. point (with error)	Flux direction	$\Phi = pe^{\frac{3r^2}{R^2}} + q_{12} \frac{r}{\sqrt{R}} \cos \vartheta e^{\frac{3r}{R}}$
•	$\vartheta = 90^\circ$	—————
◦	$\vartheta = 45^\circ$	- - - - -
+	$\vartheta = 0^\circ$	- · - · -

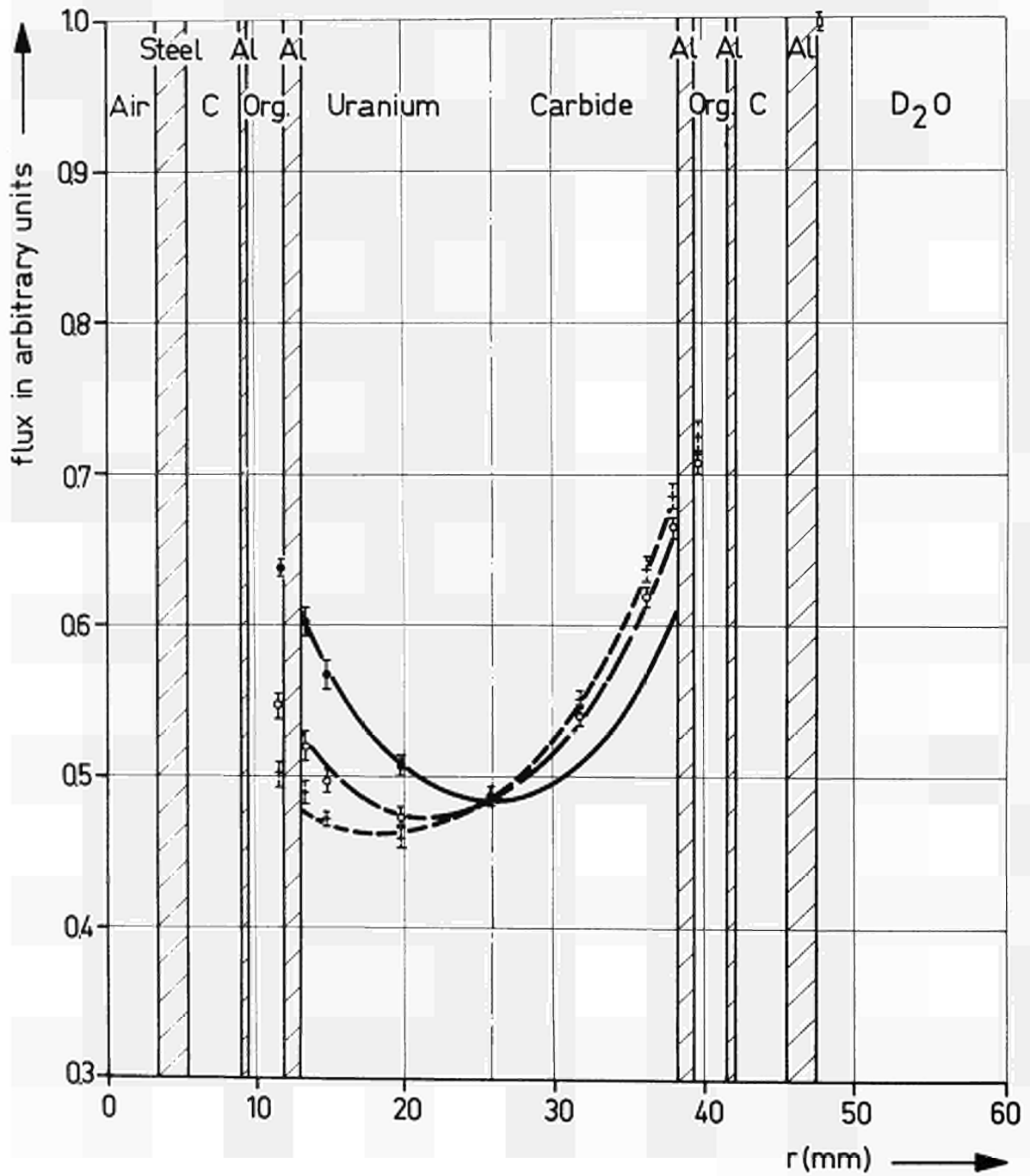


Fig.18 Fuel element:ESSOR C2 steel poisoned
Analytical thermal flux distribution

Exp. point (with error)	Flux direction	$\Phi = pe^{3r^2} + q_{1,2} \frac{r}{\sqrt{R}} \cos \theta e^{3r}$
•	$\theta = 90^\circ$	—————
◦	$\theta = 45^\circ$	- - - - -
+	$\theta = 0^\circ$	- - - - -

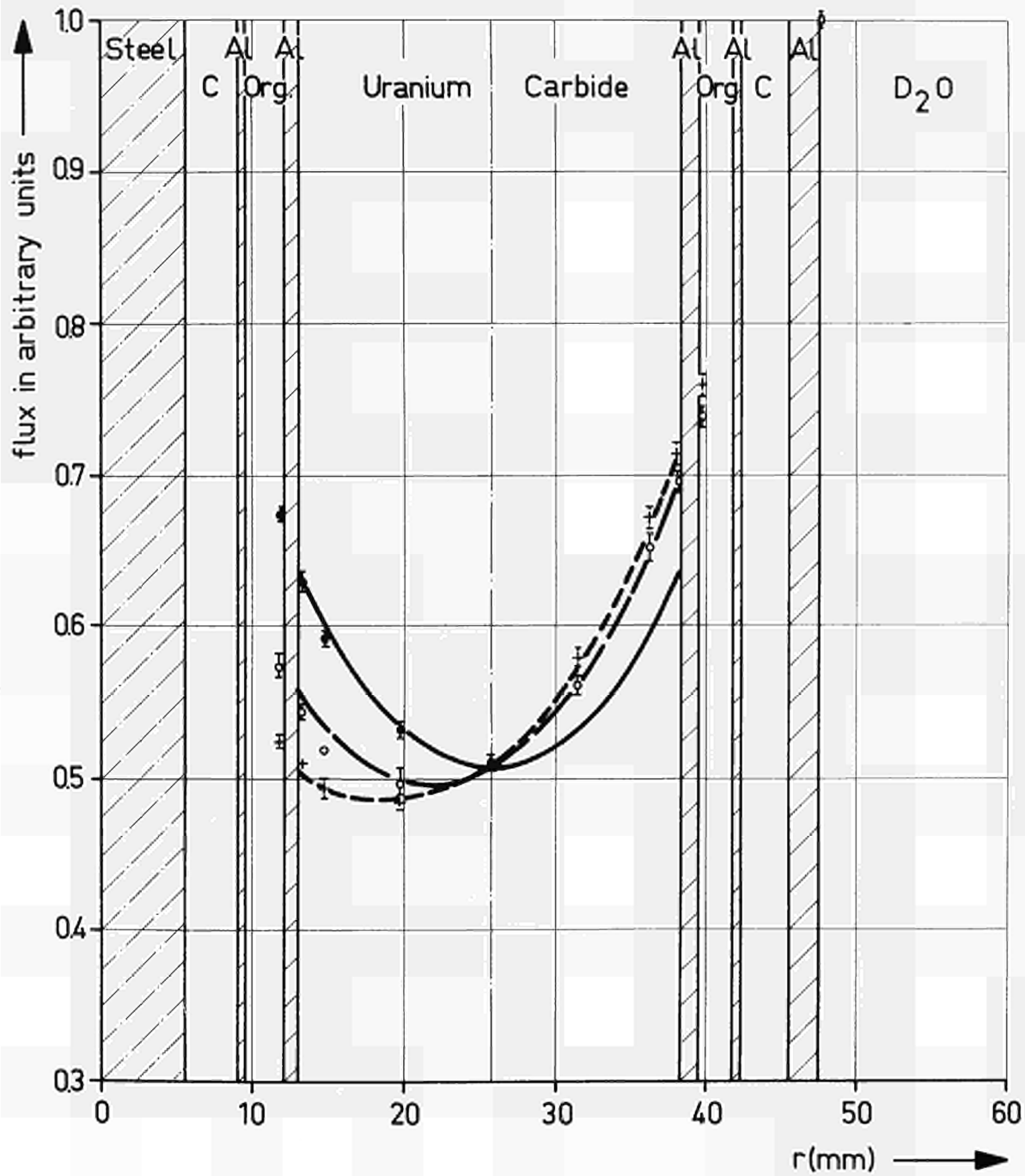


Fig. 19 ESSOR C2 nickel poisoned
Analytical thermal flux distribution

Exp. point (with error)	Flux direction	$\Phi = (pe^{3r^2} + q_{12}\frac{r}{\sqrt{R}} \cos \vartheta)e^{3r}$
•	$\vartheta = 90^\circ$	—————
◦	$\vartheta = 45^\circ$	- - - - -
+	$\vartheta = 0^\circ$	- - - - -

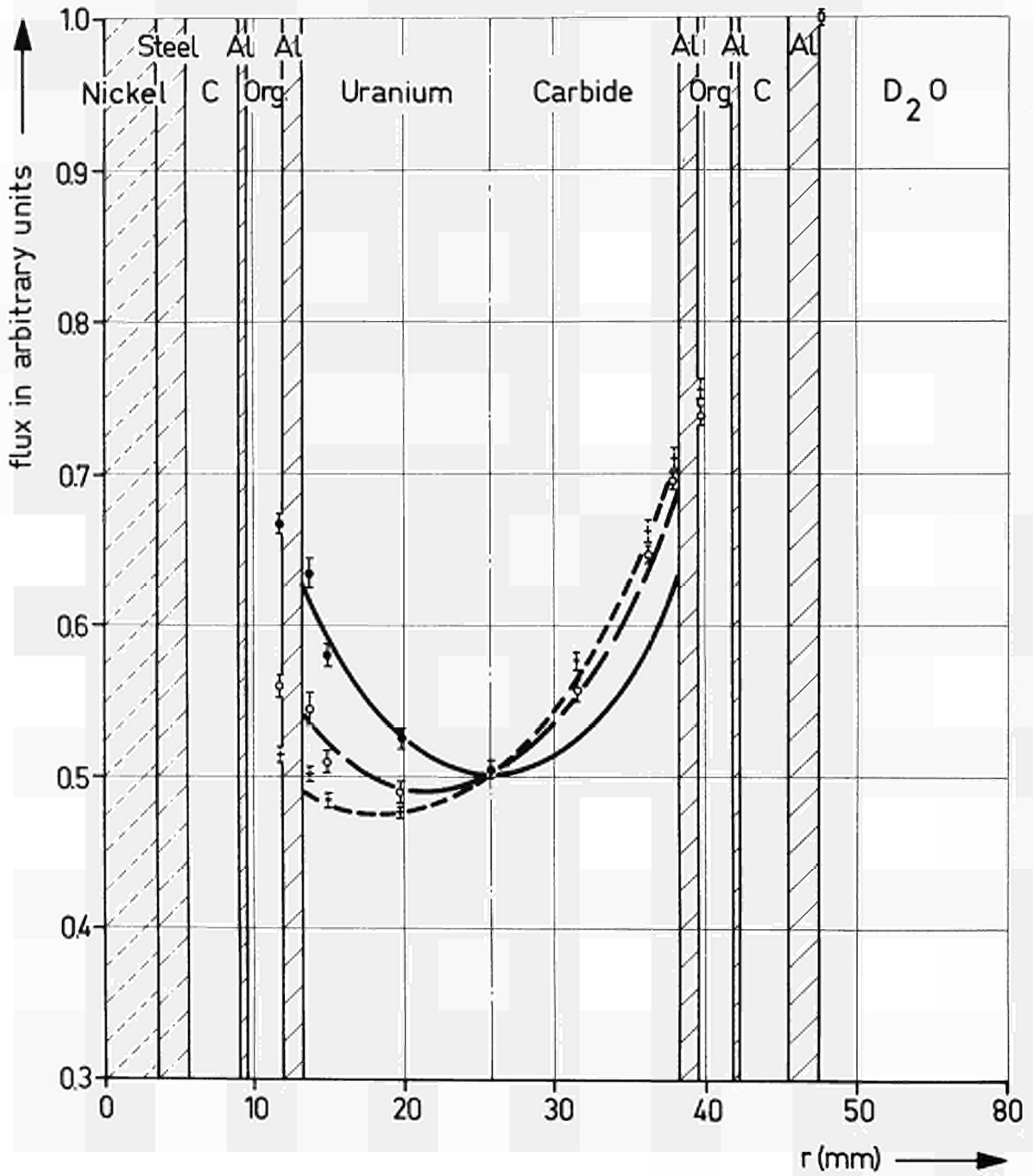


Fig. 20 Fuel element: ORGEL version of ESSOR C 2 with diphyl. Analytical thermal flux distribution

Exp. point. (with error)	Flux direction	$\Phi = pe^{3r^2} + q_{12} \frac{r}{\sqrt{R}} \cos \theta e^{3r}$
•	$\theta = 90^\circ$	—————
◦	$\theta = 45^\circ$	- - - - -
+	$\theta = 0^\circ$	- - - - -

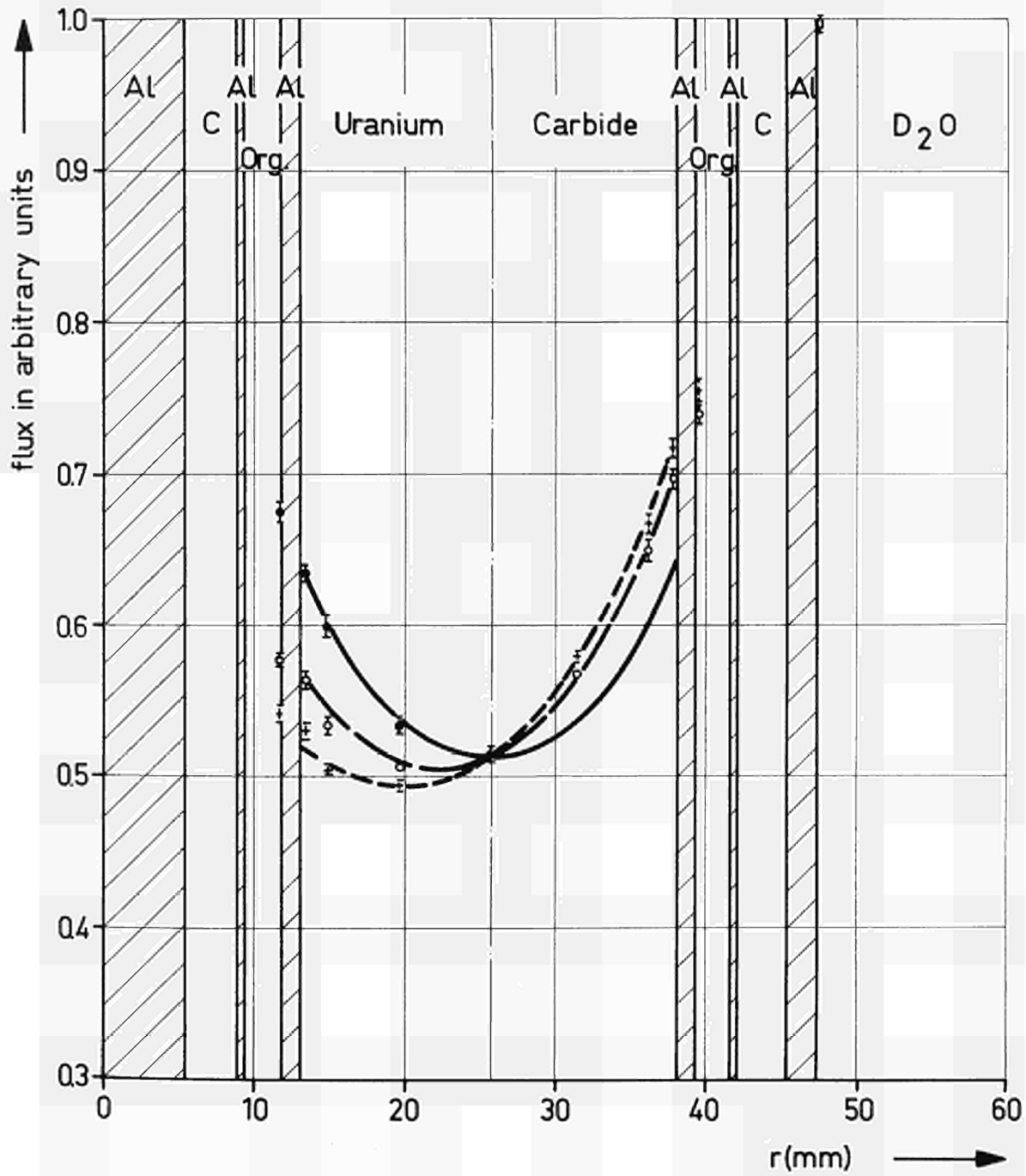


Fig. 21 Fuel element: ORGEL version of ESSOR C2 without diphyl. Analytical thermal flux distribution

Exp. point (with error)	Flux direction	$\Phi = pe^{\frac{3}{2}r^2} + q_{1,2} \frac{r}{\sqrt{R}} \cos \vartheta e^{\frac{3}{2}r^2}$
•	$\vartheta = 90^\circ$	—————
◦	$\vartheta = 45^\circ$	- - - - -
+	$\vartheta = 0^\circ$	- · - · -

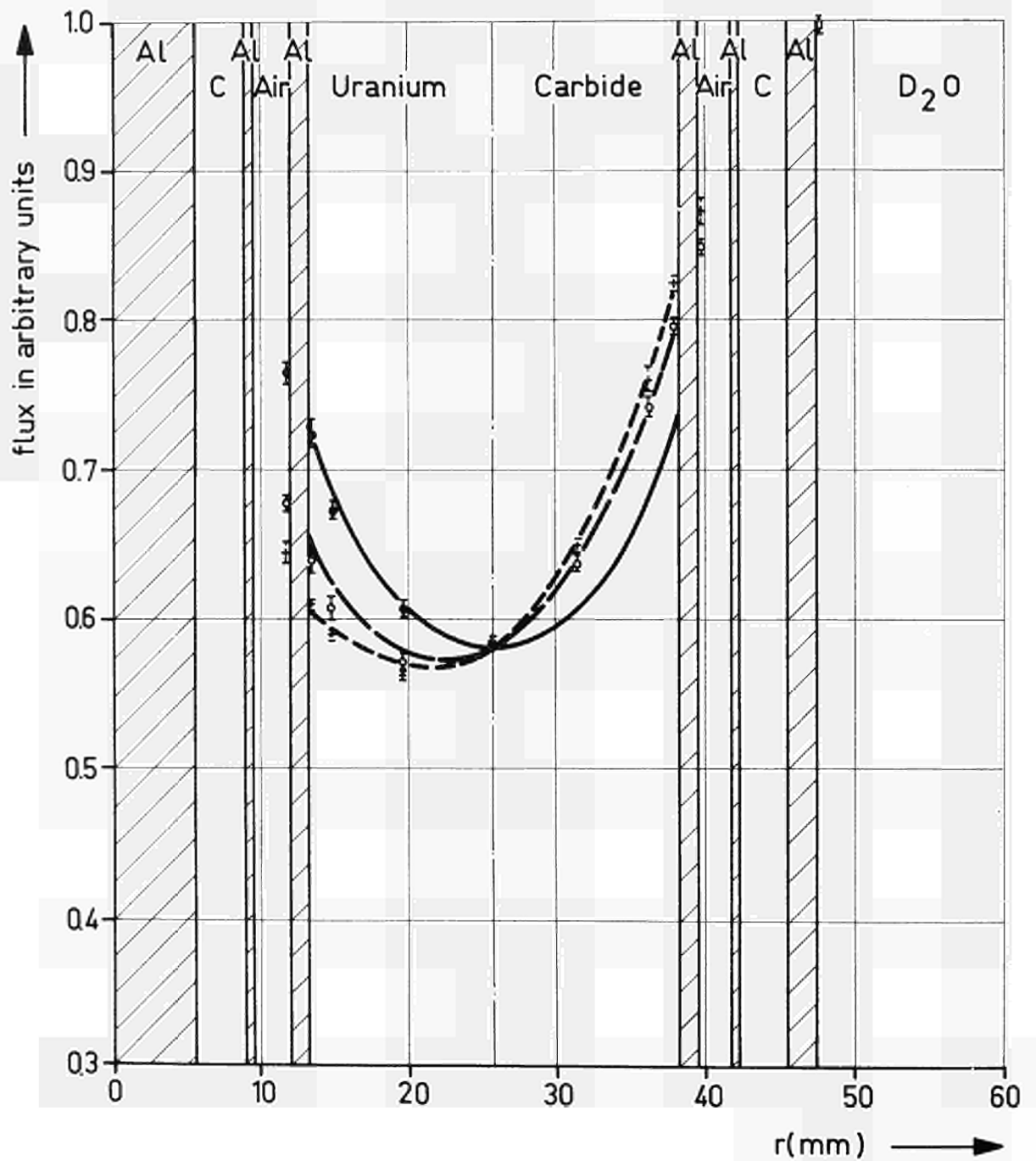


Fig. 22

Fuel element : ESSOR C2 standard
Analytical and measured thermal flux distributions

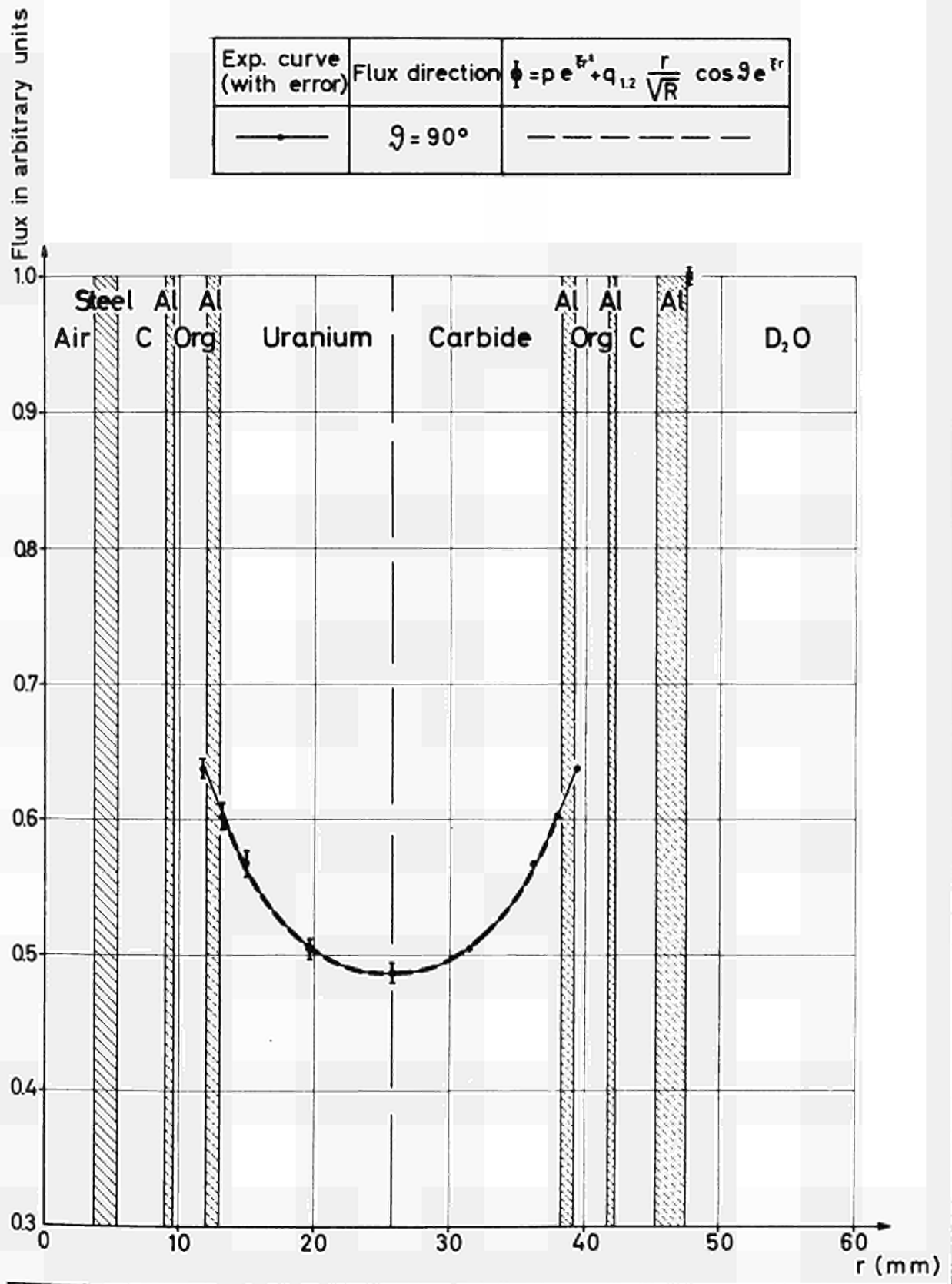


Fig. 23

Fuel element : ESSOR C2 standard

Analytical and measured thermal flux distributions

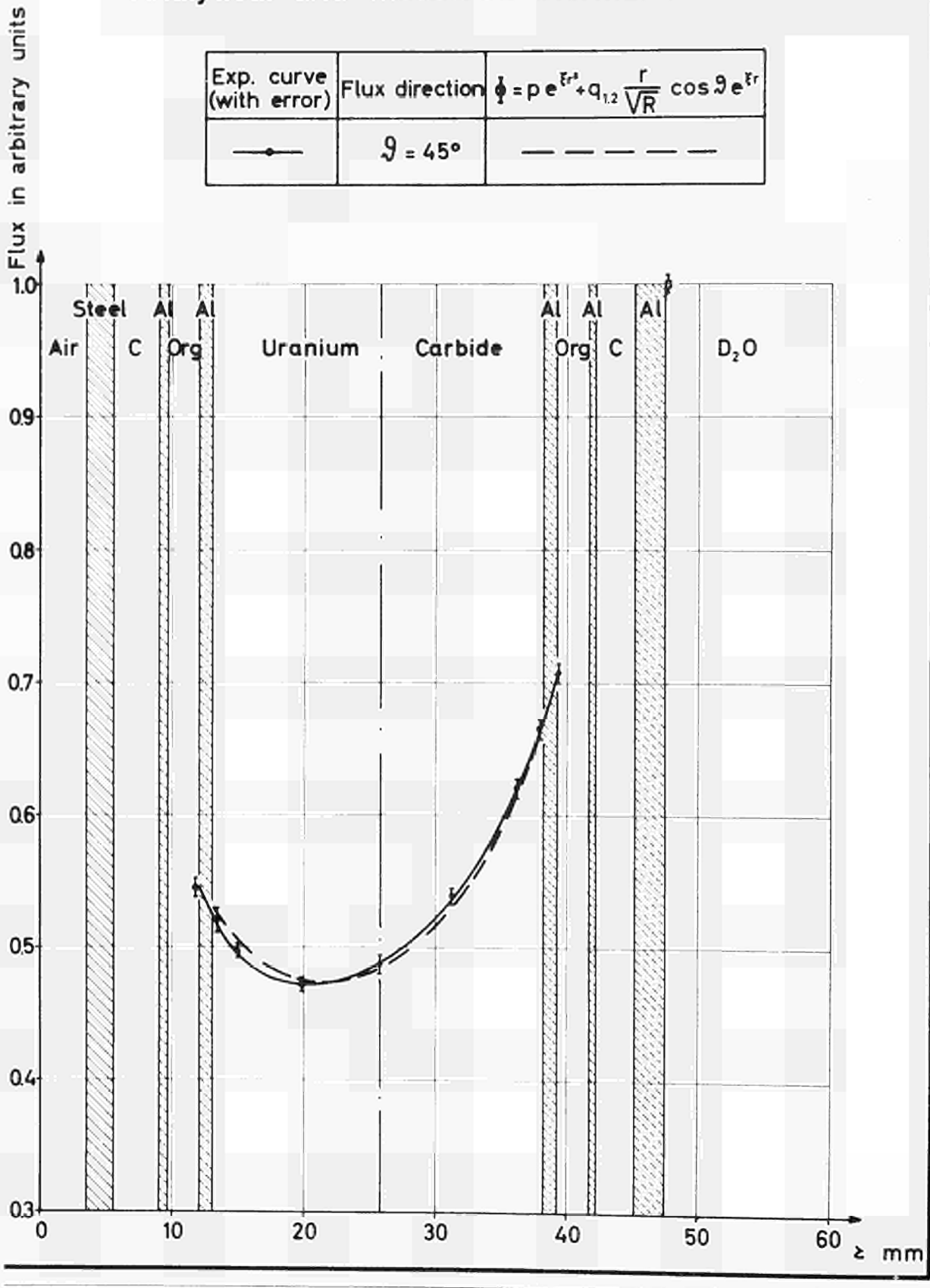
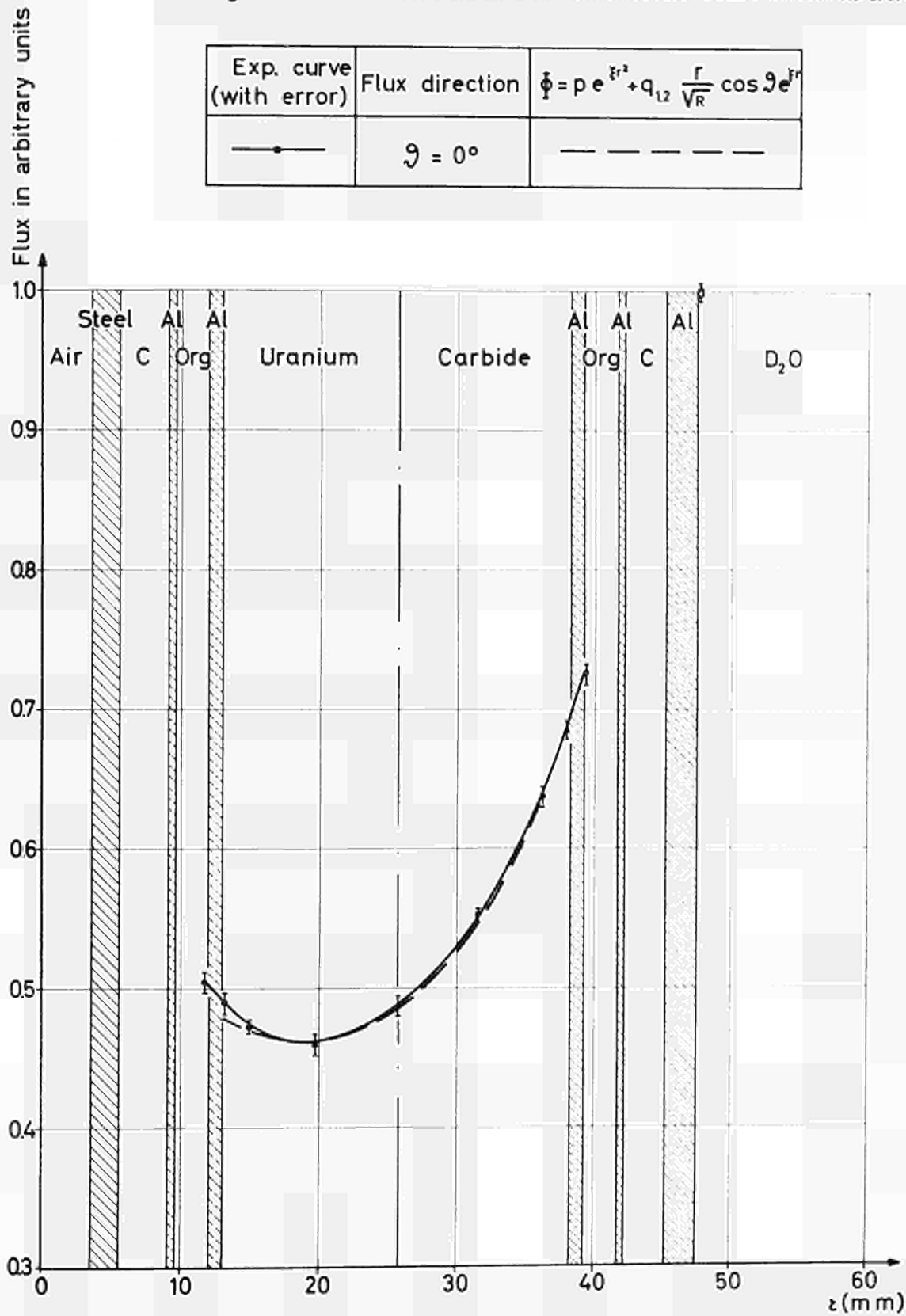
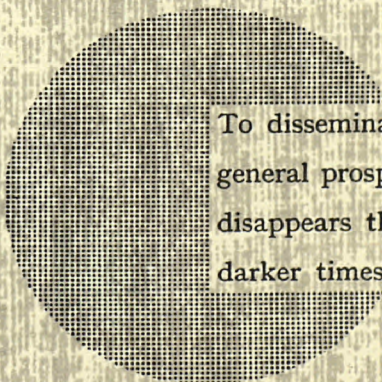


Fig.24

Fuel element: ESSOR C2 standard
Analytical and measured thermal flux distributions

Exp. curve (with error)	Flux direction	$\phi = p e^{-kr^2} + q_{12} \frac{r}{\sqrt{R}} \cos \vartheta e^{-kr}$
	$\vartheta = 0^\circ$	





To disseminate knowledge is to disseminate prosperity — I mean general prosperity and not individual riches — and with prosperity disappears the greater part of the evil which is our heritage from darker times.

Alfred Nobel

SALES OFFICES

All Euratom reports are on sale at the offices listed below, at the prices given on the back of the cover (when ordering, specify clearly the EUR number and the title of the report, which are shown on the cover).

PRESSES ACADEMIQUES EUROPEENNES

98, Chaussée de Charleroi, Bruxelles 6

Banque de la Société Générale - Bruxelles
compte N° 964.558,

Banque Belgo Congolaise - Bruxelles
compte N° 2444.141,

Compte chèque postal - Bruxelles - N° 167.37,

Belgian American Bank and Trust Company - New York
compte No. 22.186,

Lloyds Bank (Europe) Ltd. - 10 Moorgate, London E.C.2,

Postcheckkonto - Köln - Nr. 160.861.

OFFICE CENTRAL DE VENTE DES PUBLICATIONS DES COMMUNAUTES EUROPEENNES

2, place de Metz, Luxembourg (Compte chèque postal N° 191-90)

BELGIQUE — BELGIË

MONITEUR BELGE
40-42, rue de Louvain - Bruxelles
BELGISCH STAATSBLAD
Leuvenseweg 40-42 - Brussel

GRAND-DUCHE DE LUXEMBOURG

OFFICE CENTRAL DE VENTE
DES PUBLICATIONS DES
COMMUNAUTES EUROPEENNES
9, rue Goethe - Luxembourg

DEUTSCHLAND

BUNDESANZEIGER
Postfach - Köln 1

ITALIA

LIBRERIA DELLO STATO
Piazza G. Verdi, 10 - Roma

FRANCE

SÉRVIS DE VENTE EN FRANCE
DES PUBLICATIONS DES
COMMUNAUTES EUROPEENNES
26, rue Desaix - Paris 15^e

NEDERLAND

STAATSDRUKKERIJ
Christoffel Plantijnstraat - Den Haag

EURATOM — C.I.D.
51-53, rue Belliard
Bruxelles (Belgique)